RESEARCH LABORATORIES FOR THE ENGINEERING SCIENCES

SCHOOL OF ENGINEERING AND APPLIED SCIENCE

UNIVERSITY OF VIRGINIA

Charlottesville, Virginia 22901

Annual Status Report

INVESTIGATION OF DIRECT INTEGRATED OPTICS MODULATORS

Submitted to:

National Aeronautics and Space Administration
Langley Research Center
Hampton, Virginia 23665

NASA GRANT NSG 1567

Submitted by:

T. E. Batchman
Associate Professor

Report No. UVA/528171/EE80/102

March 1980

Annual Status Report

INVESTIGATION OF DIRECT INTEGRATED OPTICS MODULATORS

Submitted to:

National Aeronautics and Space Administration
Langley Research Center
Hampton, Virginia 23665

NASA GRANT NSG 1567

Submitted by:

T. E. Batchman
Associate Professor

Department of Electrical Engineering
RESEARCH LABORATORIES FOR THE ENGINEERING SCIENCES
SCHOOL OF ENGINEERING AND APPLIED SCIENCE
UNIVERSITY OF VIRGINIA
CHARLOTTESVILLE, VIRGINIA

Report No. UVA/528171/EE80/102 Copy No. 2
March 1980

TABLE OF CONTENTS

		page
SUMMARY		1
I.	INTRODUCTION	2
II.	INVESTIGATION OF MODULATION CONCEPTS	5
	A. Photoconductive Devices	6
	1. Waveguide solutions	8
	2. Organic conductors	12
	B. MOM Devices	13
	C. PROM and Other Devices	20
III.	SEMICONDUCTOR-CLAD OPTICAL WAVEGUIDES	22
	A. Variations of Conductivity	22
	B. Selection of Cladding Thickness	25
	C. Material Selection	33
	D. Conclusions	42
IV.	FABRICATION OF ION EXCHANGED WAVEGUIDES	47
V.	PROPOSED EXPERIMENTAL DEVICES	50
	A. Verification Experiments	53
	B. The Phase Modulator	55
VI.	REFERENCES	56
APPENDIX A - PUBLICATIONS		A-1

SUMMARY

The purpose of this program is to study direct modulation techniques applicable to integrated optics data preprocessors. Several methods of modulating a coherent optical beam by interaction with an incoherent beam have been studied. It was decided to investigate photon induced conductivity changes in thin semiconductor cladding layers on optical waveguides. Preliminary calculations indicate significant changes can be produced in the phase shift in a propagating wave when the conductivity is changed by ten percent or more. Experimental devices to verify these predicted phase changes are currently being fabricated and experiments are being designed to prove the concept.

I. INTRODUCTION

An integrated optics holographic comparator has been proposed [1] for use as a data preprocessor for airborne optical sensors. This device, as presently proposed, requires the conversion of the sensor optical signal into an electrical signal which then modulates a coherent optical beam by means of a set of metal electrodes deposited on a lithium niobate waveguide (Figure 1). This technique introduces noise and extra hardware because of the needed signal conversion from optical to electrical.

The objective of this investigation is to determine the feasibility of direct modulation of a coherent optical beam by an incoherent optical source to eliminate some of the above problems. Several direct modulation techniques have been investigated during the first half of this study. One technique investigated was the metal-barrier-metal, or more commonly metal-oxide-metal device (MOM), which makes use of tunneling effects through a barrier region. While the MOM device shows great promise for this application it is still in the early stages of research and its ability as an optical modulator in an integrated optical circuit has yet to be investigated. This device will be discussed in Section 2.

Two other tecniques currently being developed are the Pockels-Readout-Optical-Modulator type memory and display devices (PROM) and a spatial light modulator being developed by M.I.T. These are also briefly discussed in Section 2.

Another concept investigated is that of a photon induced change in conductivity in a semiconductor clad optical waveguide. This has been investigated theoretically in Section 3. It is shown that conductivity

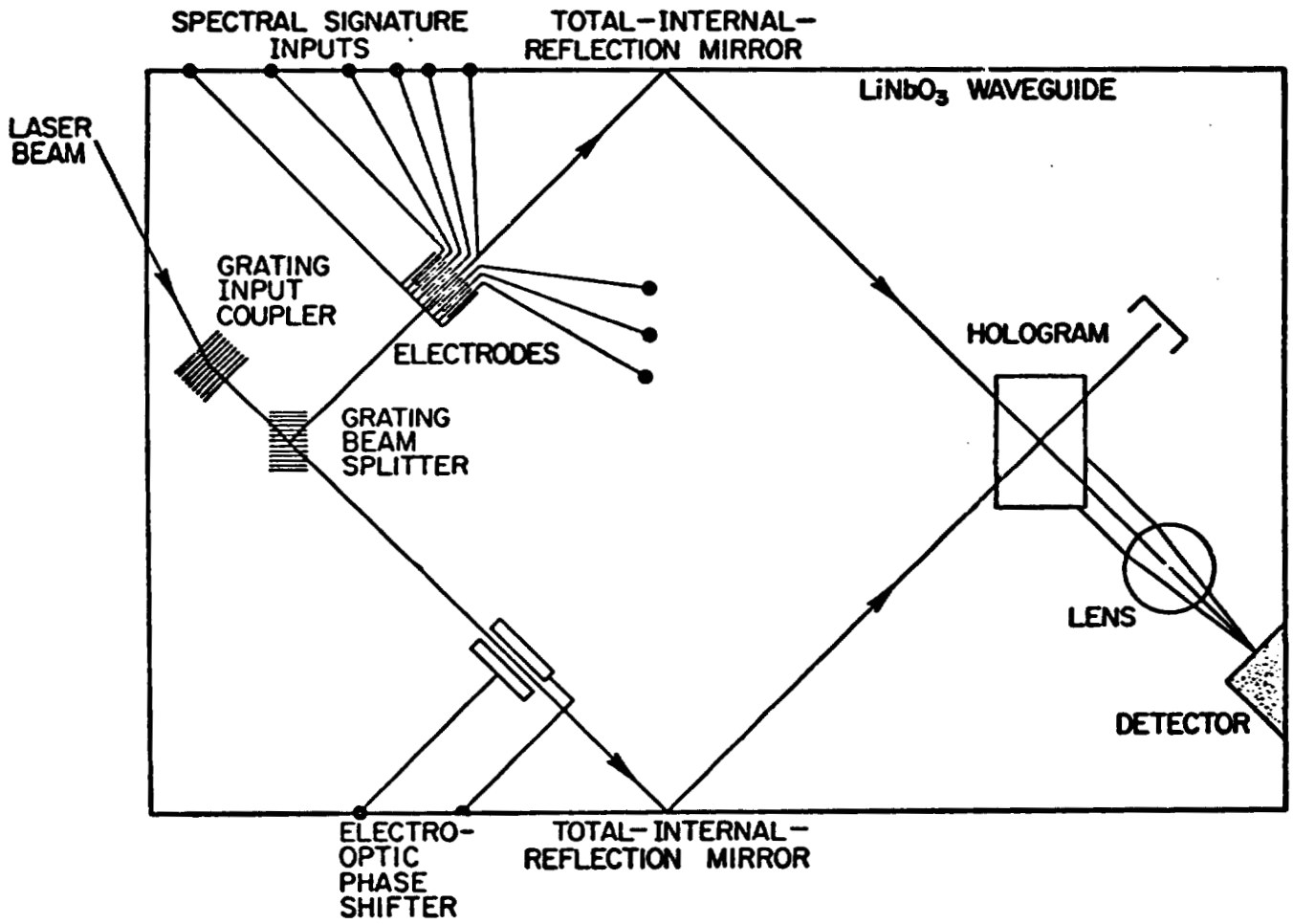

FIGURE 1. SCHEMATIC OF ONE CONFIGURATION OF THE INTEGRATED OPTICS HOLOGRAPHIC COMPARATOR. (REF. 1)

changes as small as ± 10% can produce a significant change in both the attenuation and phase constants of an optical wave propagating in the waveguide. Closer investigation has shown that these effects can be maximized by proper choice of the thickness of the semiconductor. It is further shown that only certain semiconductors (GaAs and Si) produce the desired effect.

Based on the predictions discussed in Section 3, an experimental device is proposed in Section 4 for verification of the predicted data. Should this experiment prove successful, an optical modulator would be built and such a device is also discussed in Section 4.

II. INVESTIGATION OF MODULATION CONCEPTS

Various modulation techniques have been investigated in a previous study by Battelle Colombus Laboratories.[2] This included a survey of the physical phenomena which might be utilized in a modulator, including photorefractive, photochromic, thermo-optic, photoconductive, and photovoltaic effects. We have concentrated our studies principally in two areas, photoconductive and metal-barrier-metal devices, while keeping abreast of new developments in other areas such as photorefractive devices.

During this study of direct modulation concepts we have not limited our scope by any particular type optical sensor which might be providing the modulation signal. In order to bound the problem somewhat we have assumed that such a modulation device would have to respond to a one-dimensional variation of intensity and that such variation would occur relatively slow in the time domain. Any device which could respond within a millisecond was considered feasible. It was also assumed the sensor had a 4 inch diameter optical system with a 1° field-of-view observing the earth. Based on data in reference 3 we estimated an earth radiance between .02 and 200 u watts cm^2 sr^1 μm^1 at a wavelength of 1 μm. This produced a photon flux of 10^{14} to 10^{19} photons/sec^{-1} μm^{-1} on the modulating element. These numbers will be used as guidelines for calculation purposes until addtional data is supplied by NASA.

The two concepts which initially seemed promising for use in a modulator were the tunneling effect in a metal-barrier-metal device (MOM) and photoconductive effects produced in semiconductor-clad-optical waveguides. These two concepts are discussed in detail below. Brief

surveys of recent developments in photorefractive devices and also the new microchannel spatial light modulator being developed by M.I.T. are also included in this section.

A. Photo Conductive Devices

Modulation effects can be produced in an optical waveguide by changing the conductivity of the waveguide or changing the conductivity of a cladding layer. Configurations for these techniques are shown in Figure 2. We have concentrated our investigations on the clad waveguide configuration since it seems to have a number of advantages. With this configuration the cladding material need not be transparent to the wavelength of light propagating in the waveguide. This allows a greater range of materials which may be used. For example, silicon and germanium are not transparent at 632.8 nm but can still be used as a cladding layer over short distances. A second reason for using the clad waveguide is that fabrication techniques would likely be much simpler since the waveguide material is not changed, only the cladding layer.

In section 3 we will discuss the selection of materials for this cladding region and how the material affects the propagation in the waveguide. It will be shown that both silicon and gallium arsenide have potential for use as a modulator whereas germanium and similar materials do not appear as promising. Organic photoconductors have been receiving attention in the literature recently because of the ability to vary the conductivety from that of a semiconductor to that of a conductor. Investigation of these materials for use in the cladding region has been initiated and will be discussed briefly.

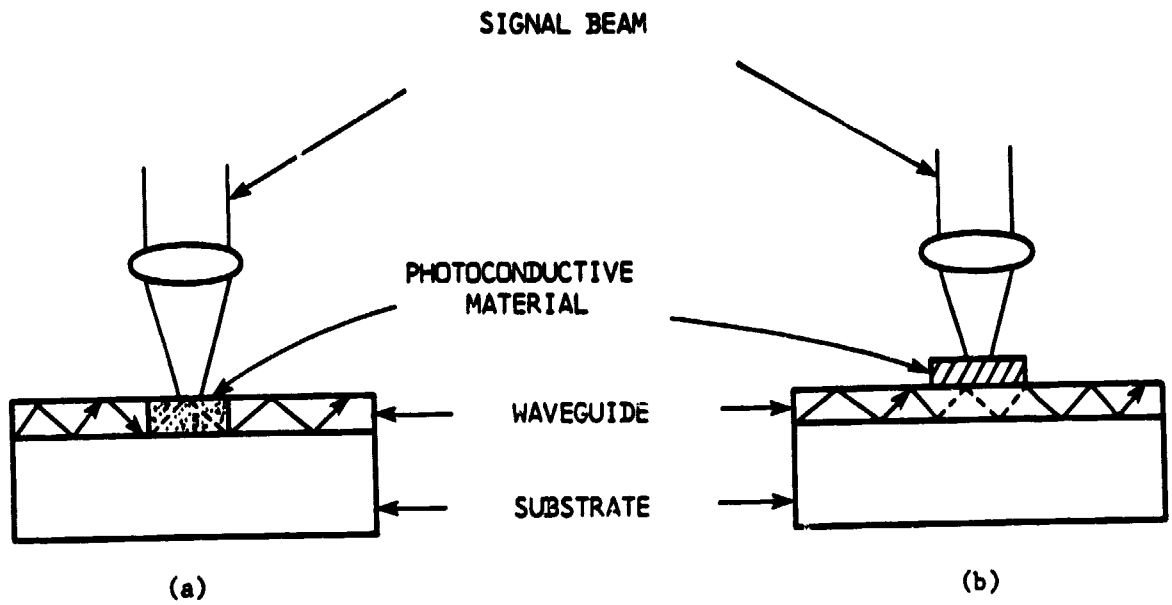

FIGURE 2. (a) PHOTOCONDUCTIVE WAVEGUIDE
(b) PHOTOCONDUCTIVE CLADDING LAYER

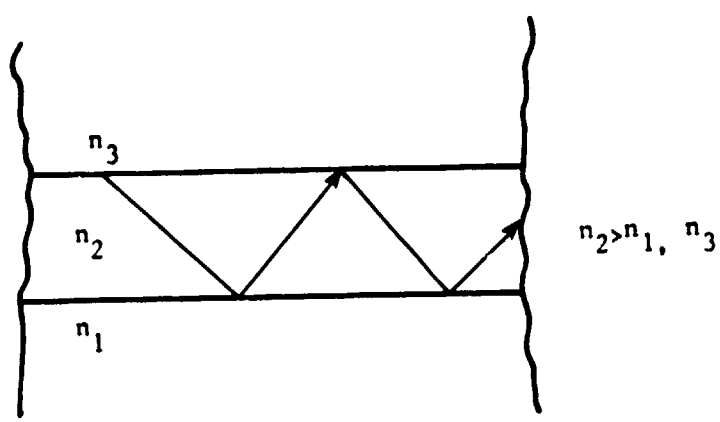

FIGURE 3. SIMPLE OPTICAL WAVEGUIDE

1. Waveguide Solutions:

We will begin our discussion of the photoconductive modulator with a brief discussion of optical waveguides and the methods we are using to determine the characteristics of waveguides of interest here. The principle of operation of integrated optical waveguides is basically simple. If light is introduced into the guiding region (n_2) at the correct angle (Figure 3), it will travel down the waveguide until it strikes a boundary with one of the surrounding layers (n_1 or n_3). Because the index of refraction of the surrounding layer is less than that of the guiding region, the light is totally reflected (Snell's Law) and continues traveling through the guiding region until it strikes another boundary producing a "zig-zag" path as shown in Fig. 3.

In traveling through the waveguide the light may follow one of many paths. Each discrete path is called a mode and is classified as either TE (transverse electric) or TM (transverse magnetic). A TE mode has no component of electrical field in the direction of propagation while a TM mode has no component of magnetic field in the direction of propagation. The TE and TM modes are further catagorized as TE_N and TM_N, where N is defined to be the mode order.

These propagading modes have a set of fields characterized by

$$\bar{E} = \bar{E}_{xyz} e^{j\omega t - \gamma z}$$

$$\bar{H} = \bar{H}_{xyz} e^{j\omega t - \gamma z}$$

where $\gamma = \alpha + j\beta$, propagation constant

ω = radian frequency of propagating wave

α = attenuation constant (nepers/meter)

β = phase constant (radians/meter)

Each mode is characterized by its own propagation constants alpha (α) and beta (β).

In order to find alpha and beta, a characteristic equation (dispersion relation[1]) must be derived and solved [4]. As Fig. 2 indicates the modulator appears as a four layer waveguide. The photoconductive material can either be on top of the waveguide as shown in Fig.2 or between the waveguide and the substrate as shown in Fig. 4.

The dispersion relation for a four-layer semiconductor-clad optical waveguide has been derived[5] using Maxwell's field equations. Rather than rederive the relation, a brief summary of the procedure followed is presented.

1. It is assumed that all materials except the semiconductor are approximately lossless and that propagation is in the z direction.
2. The non-zero field components of the TE and TM modes are determined and substituted into the wave equation.
3. The wave function is obtained by solving the wave equation. By invoking the condition of continuity of the wave function and by forcing the field components to satisfy Maxwell's boundary conditions, the dispersion relation is obtained:

$$K_{x3}t_3 = \tan^{-1}\left[\frac{K_{31}\frac{P_{x1}}{K_{x3}} + K_{32}\frac{P_{x2}}{K_{x3}}\tanh P_{x2}t_2}{1 - K_{21}\frac{P_{x1}}{P_{x2}}\tanh P_{x2}t2}\right] + \tan^{-1}\frac{K_{34}P_{x4}}{K_{x3}} + N\pi \quad (1)$$

where $K_{ij} = 1$ for TE modes

$K_{ij} = \varepsilon_i/\varepsilon_j$ for TM modes

$P_{xi} = \left[(\beta^2 - \alpha^2 - \varepsilon_i' K_o^2) + j(\varepsilon_i'' K_o^2 \quad 2\alpha\beta)\right]^{\frac{1}{2}}$

$K_{xi} = \left[(\varepsilon_i' K_o^2 - \beta^2 + \alpha^2) + j(2\alpha\beta - \varepsilon_i'' K_o^2)\right]^{\frac{1}{2}}$

$N = 0,1,2,\ldots.$ = mode order

[1]A dispersion relation is any functional equation which relates the modal propagation constants to the frequency of the wave and the waveguide parameters, such as thickness and permittivity.

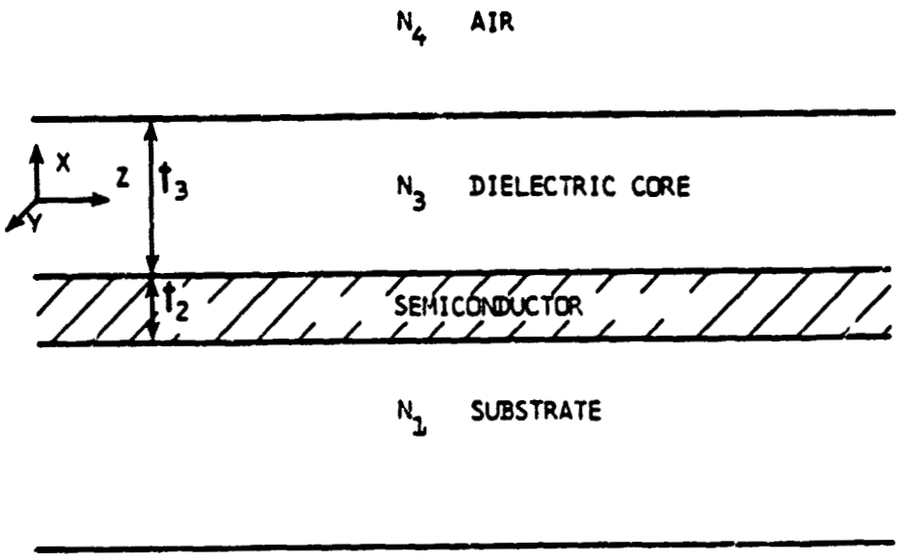

FIGURE 4 FOUR LAYER WAVEGUIDE CONFIGURATION

$K_o = 2\pi/\lambda$

$\varepsilon_i = \varepsilon_i' - j\varepsilon_i''$ = complex permittivity of region i.

This is not only a transcendental equation but it also involves the complex arctangents and the complex hyberbolic tangents. The only practical method of solving the dispersion relation is by use of a computer. A computer program has evolved over a period of eight years for solving the dispersion relation. This program employs the razor search method developed by Bandler and Macdonald[6] for optimization of microwave networks.

The razor search method requires the operator to select initial values of alpha and beta. The computer then conducts pattern searches around these points until a combination of alpha and beta satisfying the dispersion relation is found. Use of the program requires such data input as layer thicknesses and permitivities, mode type and mode order, wavelength, the initial "guess" of alpha and beta, and various convergence factors used in determining when a suitable alpha and beta have been found.

Initially the program set up was such that the thickness of the second layer (the semiconductor layer) remained constant while that of the third layer (the guiding region) was allowed to vary. In order to obtain additional characteristics of waveguides the program has been modified so that the thickness of the guiding region remains constant while that of the metal cladding varies.

At optical frequencies the complex permittivety is related to the conductivity (σ) as follows:

$$\varepsilon'' = \frac{4\pi\sigma}{\omega}$$

This conductivity can be changed by incident photons in semiconductors and in certain inorganic materials. In a semiconductor the conductivity is given by

$$\sigma = \sigma_o + e\,\Delta n\,(\mu_p + \mu_n) \qquad (3)$$

σ_o = conductivity of sample without light.
e = charge on electron.
μ_p, μ_n, = mobility of holes and electrons.
Δn, Δp = changes in concentration of free carriers due to incident light.

To maximize the change in conductivity we need to keep σ_o as low as possible. This can be done using high resistivity semiconductors. Large changes in conductivity have been observed in silicon illuminated with a pulsed laser.[7,8,9] Conductance changes from 10^{-4} (ohm cm)$^{-1}$ to 10^{3} (ohm cm)$^{-1}$ were observed when illuminated with a 100 watt laser.

This optically produced change in conductivity will affect the attenuation and phase constants of the propagating modes in the four-layer waveguide according to equation (1). It has been generally concluded[1] that this effect is small at the levels of incident radiation expected on the airborne receiver. In Section 3 we will show that under proper conditions the effect can be maximized to the point where it could be used in a direct modulator.

2. Organic Conductors:

Within the last two years several research organizations have been developing organic photo conductors[10,11,12,13] for use in recording films and solar energy converters. Currently there are four materials which have been receiving attention: $(SN)_x$, polyacetylene, polyparaphenylene and polyprrole. These electrically conducting polymers have

been induced to show a range of conductivities, from values of insulators, through those of semiconductors and almost as far as the quantities possessed by metals.

The electrical conductivity can be varied over 10 to 12 orders of magnitude by doping in some cases or by copolymerizing with closely related polymers. Presently we have not found sufficient published data on the photconductivity of these materials to evaluate them for use in modulators. However, the feeling among some chemists is that the quantum efficiency for photon conversion will be high.

B. MOM Devices

Metal-Oxide-Metal Devices (MOMs) exhibiting an invariant I-V characteristic extending from dc up to optical frequencies have been fabricated and tested as the University of California.[16] Fabricated devices have demonstrated properties of amplification, modulation and detection. The geometrical structure of the device lends itself to integrated optics, in that both utilize the same fabrication techniques and are thin film structures. However the MOMs are presently being fabricated on the back of prisms to enable optical signal coupling into and out of the devices; therefore, all operations are restricted to free space waves.

The inherent device versatility for use as active components, such as amplifiers, mixers and fast detectors, makes it attractive for use on a common integrated optical substrate. It has also been proposed that an optical transistor could be constructed which would then lead to the development of a new optical oscillator if successful coupling to a waveguide is achieved.

The metal-oxide-metal device (MOM) consists of approximately a one-to-two nanometers thick oxide placed between two metal films (Figure 5)[16]. When optical radiation is incident on the device, part of it is absorbed in the metal and part contributes to an electrical field in the oxide. Device operation is believed to be from three mechanisms [16,17,18]: Fermi level modulation by the trapped electric field in the oxide, photon assisted electron tunneling through the oxide due to phonon creation by incident photons, and direct optical excitation of electron tunneling (Figure 5). In treating the device as a waveguide, it has been found that neither TE nor TM modes will propagate through the device, since the oxide is below the cutoff thickness for symetrical metal-clad waveguides[15]; however, surface plasma modes are excited on each metal. The existence of these surface plasma modes at interfaces of metals and dielectrics has been studied [19,20,21,22,23,24]. These surface plasma modes excite gap plasma modes in the MOM device. Either symmetric or antisymmetric modes are excited, depending on whether the two surface plasma modes are in phase or out of phase by π radians. If the antisymetric mode is excited then fermi level modulation of tunneling electrons takes place. Since the oxide is so thin, transition times for tunneling electrons are on the order of 10^{-16} sec, which allows for transition frequencies up to 10^{16} Hertz or light frequencies. Even though surface plasma wave amplification mechanisms are not completely understood at this time, the process has been theorized to exist and has recently been demonstrated.

Presently, the devices are being fabricated on the back of prisms, and light is coupled into the device by excitation of the surface plasma mode on the metal film/prism interface, Figure 6A.[18] An analysis of

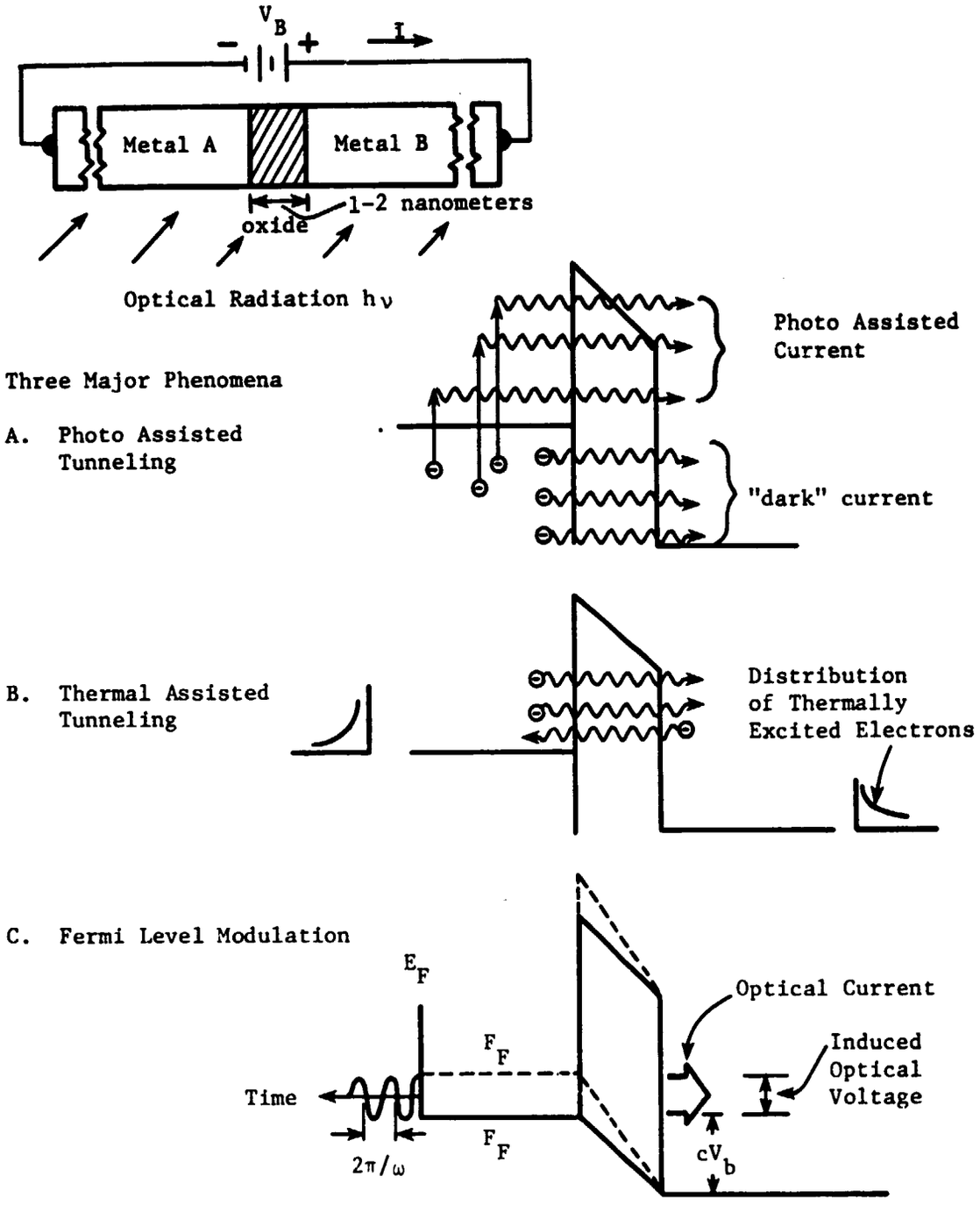

FIGURE 5. THE MECHANISMS OF PHOTO, THERMAL, AND FIELD ASSISTED TUNNELING DUE TO INCIDENT LIGHT

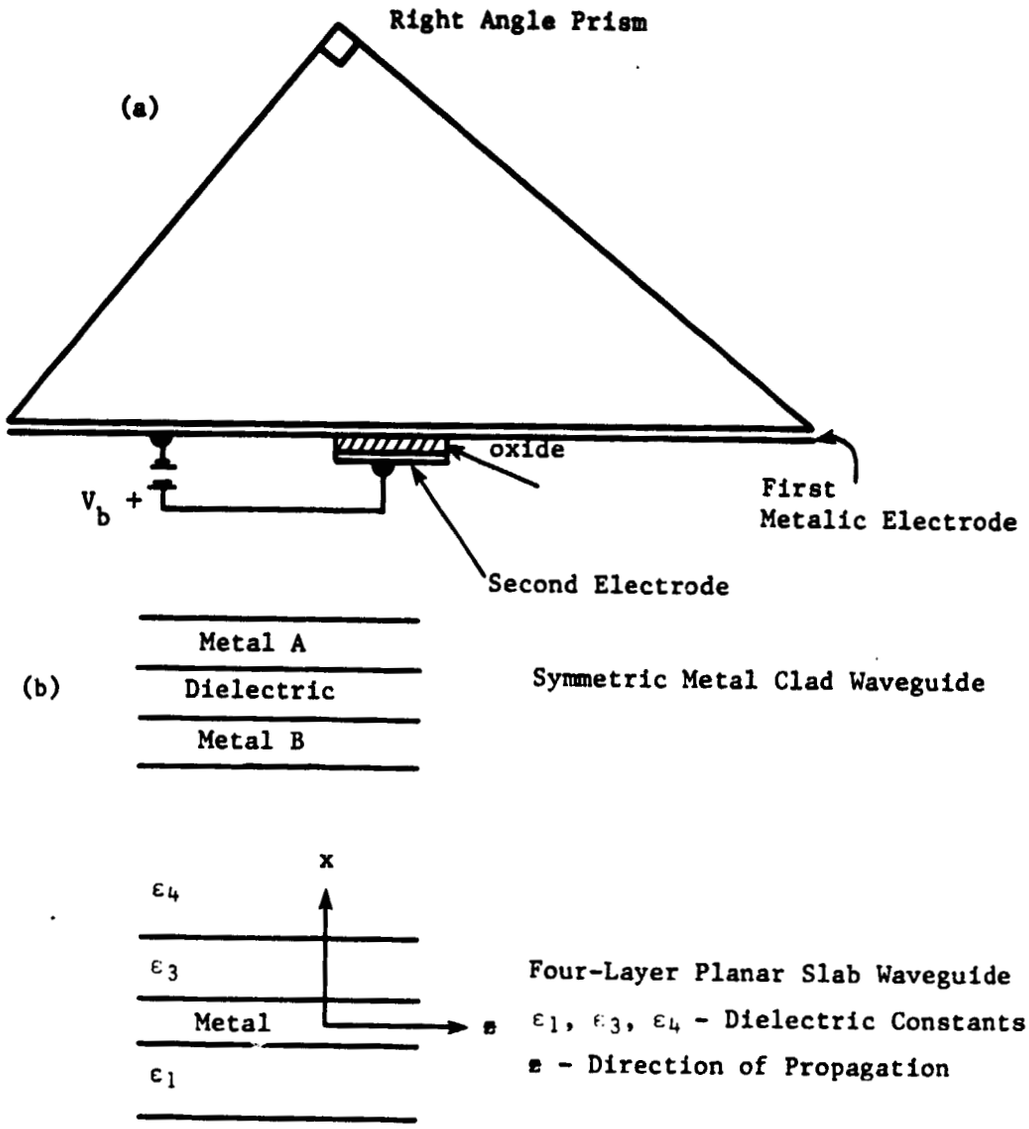

FIGURE 6. MOM DEVICE FABRICATED ON A PRISM

this coupling procedure [17,25,26,27] shows that coupling efficiencies of this method can exceed 90 percent if certain criteria are met. That is, the inclusion of a dielectric between the prism and the metal of such thickness and dielectric constant that the evanescent wave present in total reflection has the same phase velocity as that of the surface plasma wave to be excited. Gustafson indicates the losses of this coupling scheme originate from the losses in exciting the surface plasma mode due to absorption by the metal, and scattering losses at the onset of the MOM.

The device is a section of a symmetric metal clad three layer waveguide (Figure 6B) where the oxide is extremely thin. Therefore, compatibility with integrated optics and waveguide technology may be realilized. It has been suggested that MOM's can be placed on the same chip along with other integrated components and interconnecting plannar slab waveguides. The device geometry is readily adapted to use in integrated optics and a coupler would have to be developed to allow for this integration. The coupling structure studied here is a modification to a four layer waveguide, dielectric-dielectric-metal-dielectric (Figure 6c). This structure already contains one electrode, and a second electrode, may be introduced by making it a symmetrical five-layer waveguide. In such a coupler, the basic guiding dielectric core would become thinner and thinner to couple TM (transverse magnetic) modes to surface plasma modes. A careful analysis of waveguide tapering technology for coupling into plasma waves would have to be performed and prototype tapering waveguides fabricated for this analysis. Tapered couplers have been analyzed for dielectric clad waveguides [28,29] and some analysis of coupling into metal-clad tapered waveguides has been

done [30]. Otto has briefly investigated coupling into the surface wave by a TM_o mode [35]. The analysis has shown TM mode conversions occuring in tapered metal regions even with a tapered buffer layer placed between the guiding core and the metal film. Further analysis of this structure would be necessary in order to allow the inclusion of the second electrode of the MOM and maximize coupling to the surface wave.

An extensive analysis of the asymmetric four-layer waveguide (Figure 6C) and their supported propagating modes has been done [15,30, 31,32,33,34]. Various metal and semiconductor clad waveguides have been analyzed and the effects of varying waveguide parameters such as film thickness and the material permitivities on propagating modes have been established.

A comparison of the three-layer-dielectric guide and a four-layer guide with a metal film inserted between the substrate and the guiding dielectric demonstrates that the inclusion of the thin metal film changes the mode profile for TM modes appreciably, yet the effect on the TE modes is only slight. Figure 7 shows the wave function profiles for the TE_o and TE_1 modes of a three-layer waveguide. The TM mode profiles are similar and have not been shown. Figure 8 shows the field distribution after a thin metal film has been introduced between the substrate and the waveguide. The TE_o profile is only slightly changed by the silver layer, but the TM_o mode has a high field concentration in the metal film. Rashleigh[15] has hypothesized that this field concentration in the metal gives rise to the TM_o mode coupling to the surface plasma mode. This hypothesis is supported by comparing the surface wave field distribution, Figure 9, to that of Figure 8 for the TM_o mode.

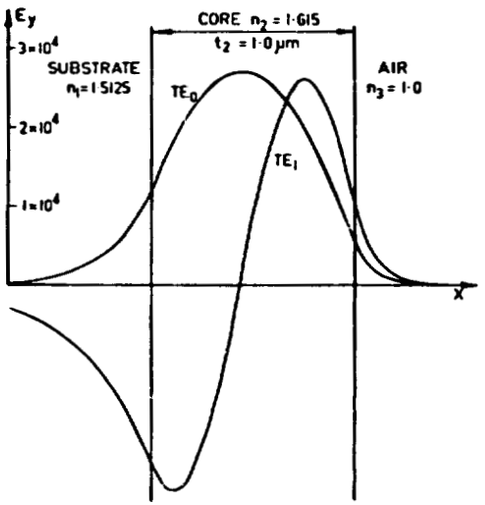

FIGURE 7. FIELD DISTRIBUTION OF DIELECTRIC CLAD WAVEGUIDE

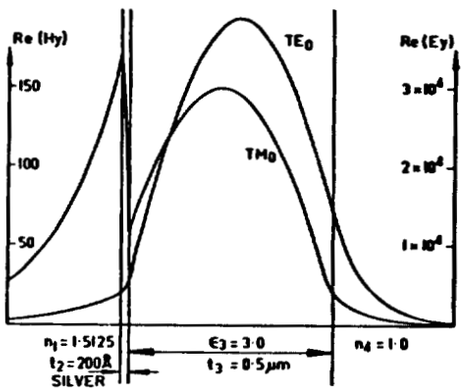

FIGURE 8. TE_0 AND TM_0 FIELD DISTRIBUTIONS AFTER INTRODUCTION OF A THIN METAL FILM

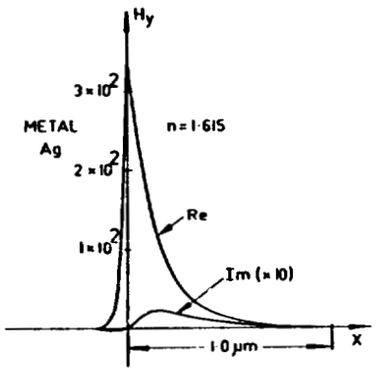

FIGURE 9. SURFACE WAVE FIELD DISTRIBUTION OF A SILVER DIELECTRIC INTERFACE

The conclusion from this analysis is that TE modes do not couple to the surface plasma modes because there is no concentration of field strength at the metal-dielectric interface where the TM' mode (surface plasma) exists. The TM mode field concentration at this interface increases as mode order is reduced. The computer solution technique mapped out previously predicts the existence of the TM' mode, in that there is extreme attenuation found in the TM modes; this is much higher than expected. The rationale is that the TM modes are coupling into a highly attenuated surface plasma mode, and thus they are highly attenuated.

From this preliminary analysis it appears feasible to build a MOM device into an integrated optical waveguide such that it could be used as a modulator. There are several serious problems which need to be investigated to determine whether it can be used in the proprosed preprocessor. No such device has ever been constructed on lithium niobate or similar materials. Also the device is in its early stages of development and its use as an optical modulator has not been explored in depth. While the MOM devices look promising in the future it would likely require several more years to develop a working device for the preprocessor application. We will continue to study this device and watch for new developments in the research program at the University of California.

C. PROM and other devices

PROM is the name given to a device being developed by ITEK [36] in which charges are trapped at an insulator-photoconductor interface. These trapped charges then affect the refractive index of a waveguide causing it to guide or become non-guiding. A similar device has been

proposed for use as a multi channel waveguide switch[37]. Battelle[2] has reviewed these devices and concluded that while they hold some promise of being applicable, the disadvantages inherent in them make it doubtful that they could be effectively used. We are continuing to survey the field and will watch work currently in progress to determine their potential for use as a preprocessor modulator.

Another device worth investigating is the micro channel spatial light modulator (MSLM) now being patented by Dr. C. Warde of Massachusetts Institute of Technology. A brief discussion in reference 38 implies that the device phase modulates a coherent beam with an incoherent beam. The MSLM is an extremely sensitive device which derives its sensitivity through a multiplication of the photon produced electrons. This would be an advantage for low light level modulation. A literature search has been initiated to gain more details on this concept. It will be reviewed again in the final report.

III. SEMICONDUCTOR - CLAD OPTICAL WAVEGUIDES

In this section we will present the results of our investigation into the effects on the attenuation and phase constants by induced photoconductivity in three common semiconductor materials. The computer program discussed in Section 2 has been used to solve the dispersion relation for the four-layer waveguide where the following parameters were allowed to vary: material conductivity was varied to investigate photoconductivity; cladding thickness (t_2) was varied to maximize changes in attenuation and phase; and the cladding material was varied to select a material producing the largest modulation effect.

Before beginning work on this grant we had observed changes in the attenuation of proagating modes in the four-layer waveguide as the cladding semiconductor material (Figure 4) was varied. For example, the real part of the complex permittivity is about the same for germanium (17.4) and gallium aisenide (14.3) but the conductivity is quite different (Ge. $\sigma = 3.21 \times 10^2$ (ohm cm)$^{-1}$ and GaAs, $\sigma = 25.4$ (ohm cm)$^{-1}$. Figure 10 shows the observed variation in attenuation for these two materials when the cladding thickness was taken as semi-infinite ($t_2 = \infty$). Although this was not a large variation in attenuation for a given guide thickness, we felt that with proper choice of material and thickness parameters we could optimize the change to make it significant.

A. Variation of Conductivity

To begin our study of this modulator we assumed that we could vary the conductivity of a semiconductor cladding by +50% and we also included a -10% variation in conductivity although a negative charge in conductivity is not likely to occur. All calculations are based on a propagation wavelength of $\lambda = 632.8$ nm. Figure 11 indicates that indeed the

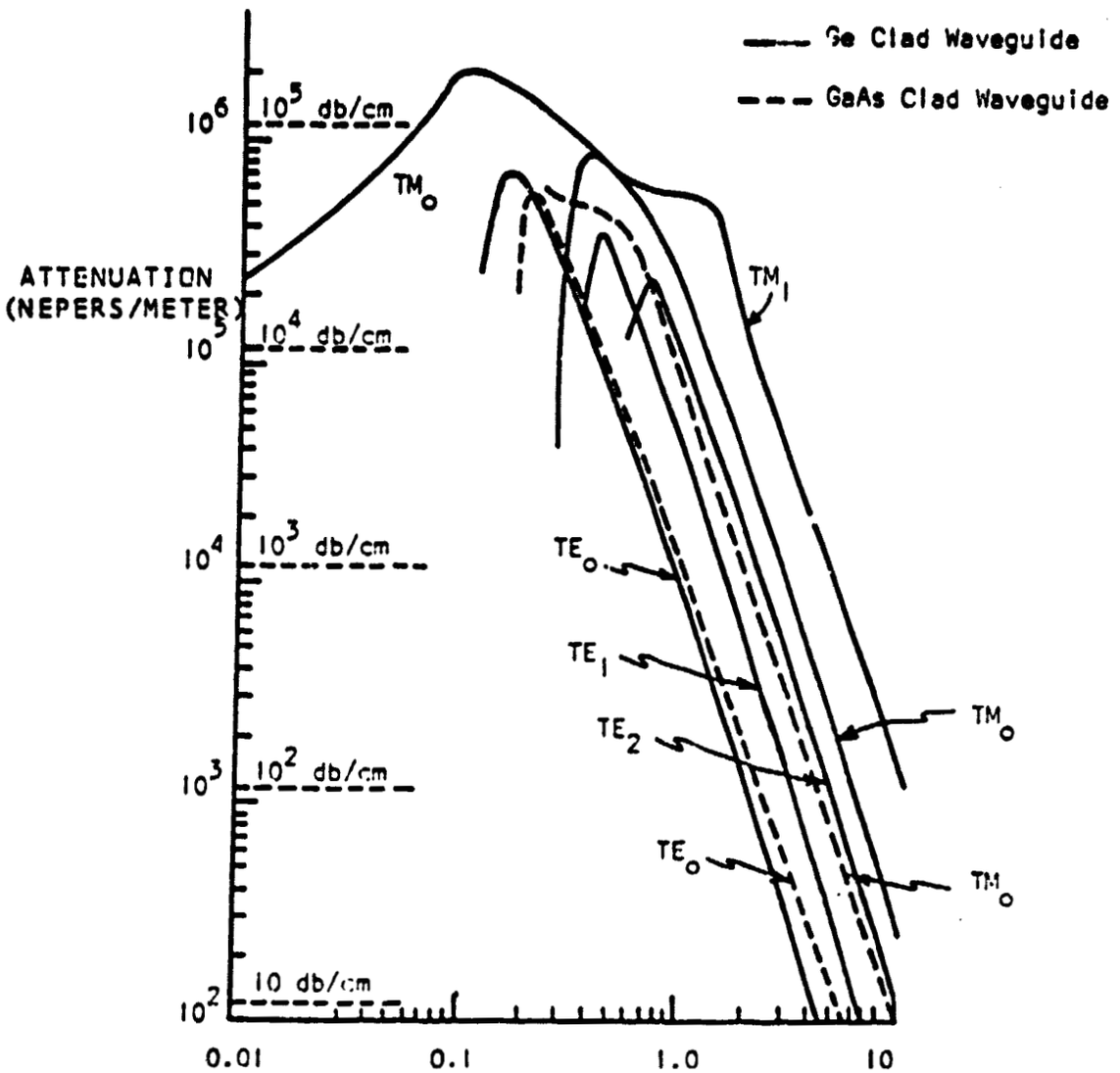

FIGURE 10. ATTENUATION OF Ge AND GaAs CLAD WAVEGUIDES

FIGURE 11. VARIATION IN ATTENUATION WITH CONDUCTIVITY FOR A GaAs CLAD WAVEGUIDE WITH t_2 = 50 nm and t_3 = 800 nm.

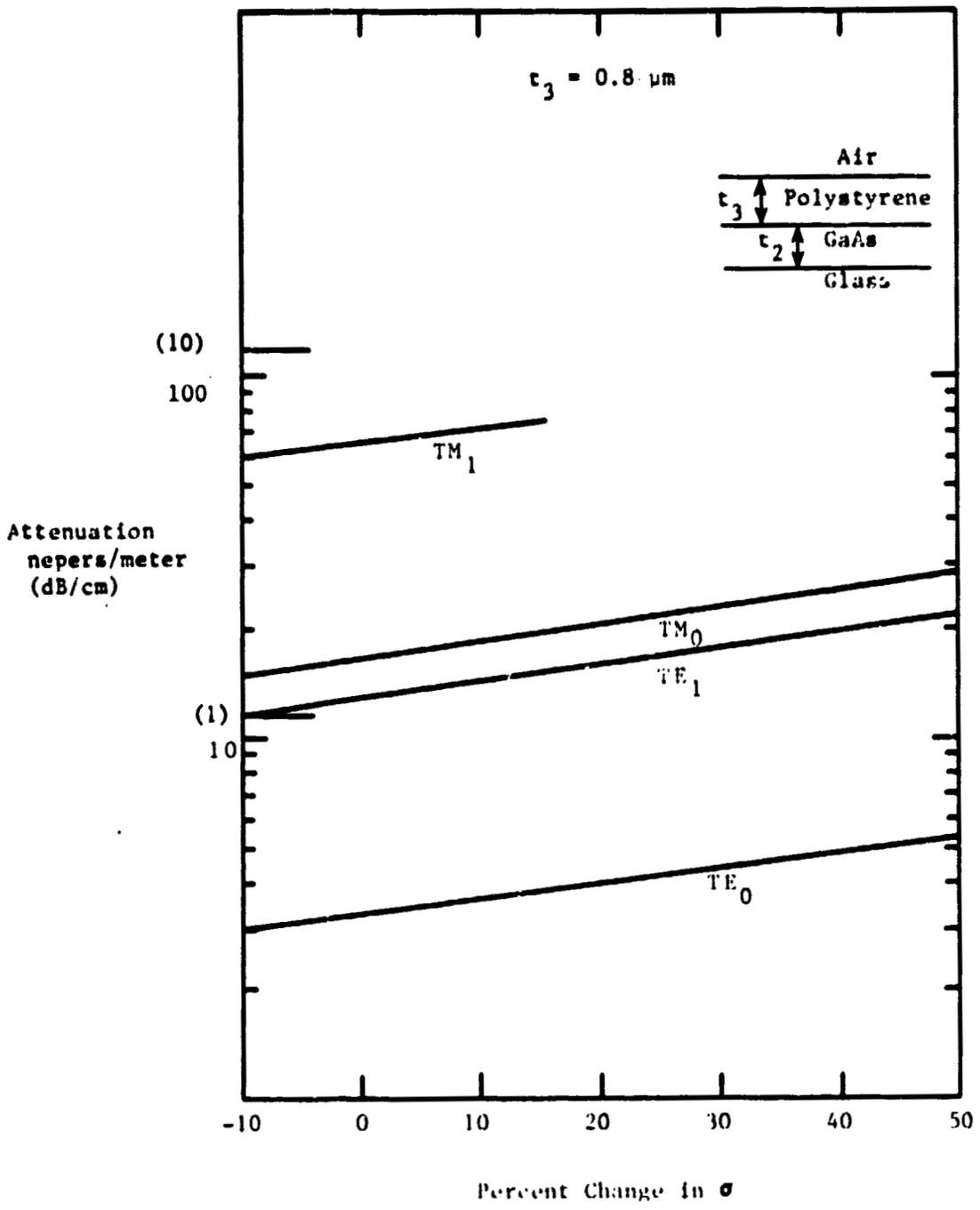

attenuation did change by at least 2dB when the conductivity of GaAs was changed by 50%. Although this is not a large change, it is significant enough to be detected. From the standpoint of the modulator for use in the holographic data preprocessor we needed a phase change. Unfortunately, the phase change was less than 1 radian/meter for this variation in conductivity.

The next step was to allow t_3 to vary to see if the waveguide thickness had any effect on the amount of change in attenuation or phase constant produced by the variations in conductivity. Figures 12 and 13 show the results of this investigation for the TE_o mode. The normalized phase constant (mode index = β/k, $k = 2\pi/\lambda$) is plotted in Figure 13 instead of the phase constant since the variations will be the same. Similiar curves were produced for the other low order TE modes and the TM modes. We see that the change in conductivity simply shifted the characteristic attenuation curve up or down in proportion to the change in conductivity. At no point did we find a change in the mode index as the waveguide thickness (t_3) was varied.

B. Selection of Cladding Thickness

Again our previous experience and published data [14] indicated that the attenuation normally decreased as the cladding thickness (t_2) was decreased. It thus seemed reasonable to vary the cladding thickness while also varying the conductivity to see if this had any beneficial results. We were perplexed at the results obtained since they were entirely different than anything previously observed. Figures 14 and 15 show the results for the GaAs clad waveguide as t_2 is varied. Not only does the attenuation and phase vary with conductivity but it also seems to oscillate after the cladding thickness decreases past 1.0 μm. This

FIGURE 12. ATTENUATION OF THE TE_0 MODE FOR A GaAs CLAD WAVEGUIDE (t_2 = 50 nm)

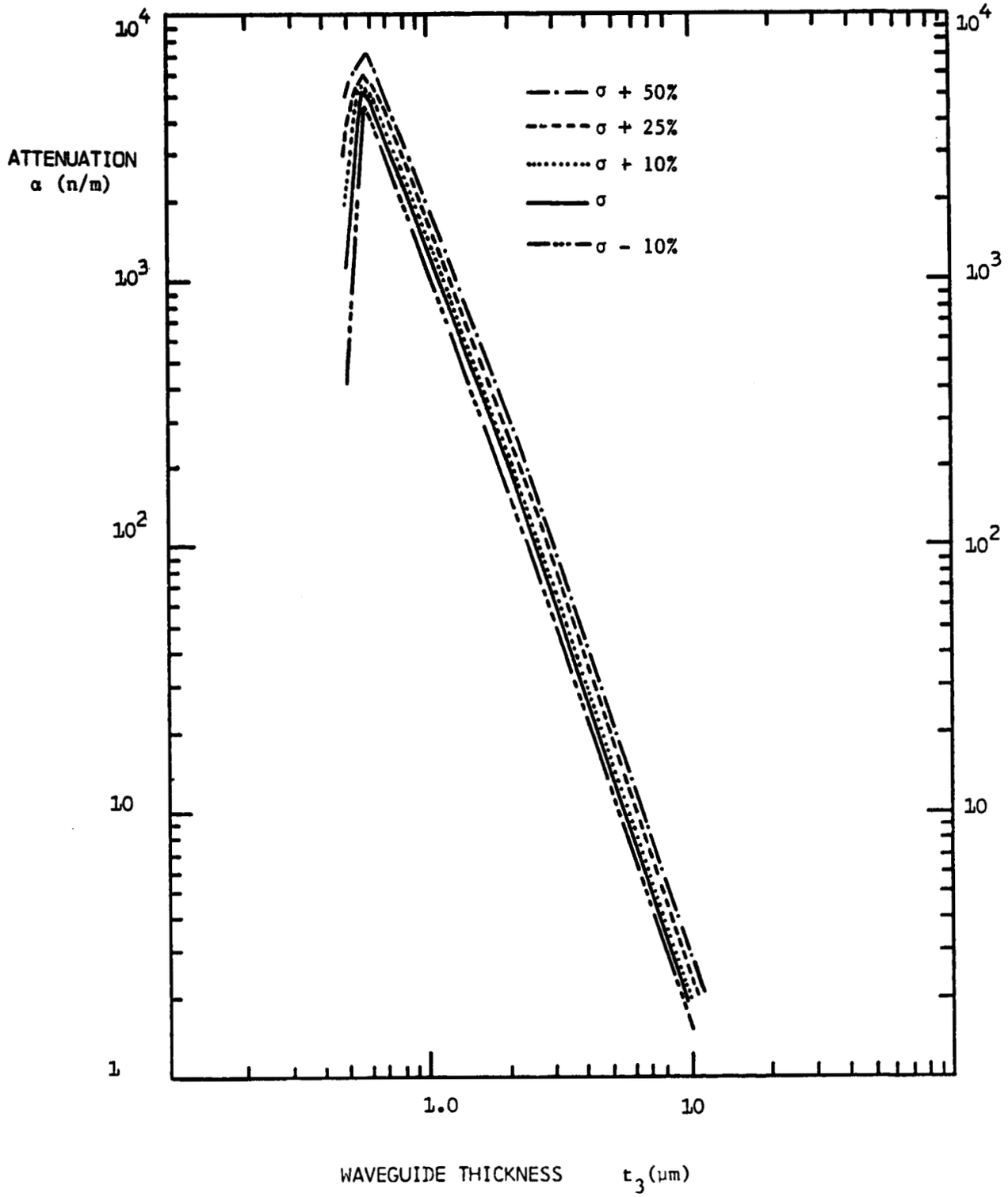

FIGURE 13. MODE INDEX OF THE TE_o MODE FOR A GaAs CLAD WAVEGUIDE (t_2 = 50nm)

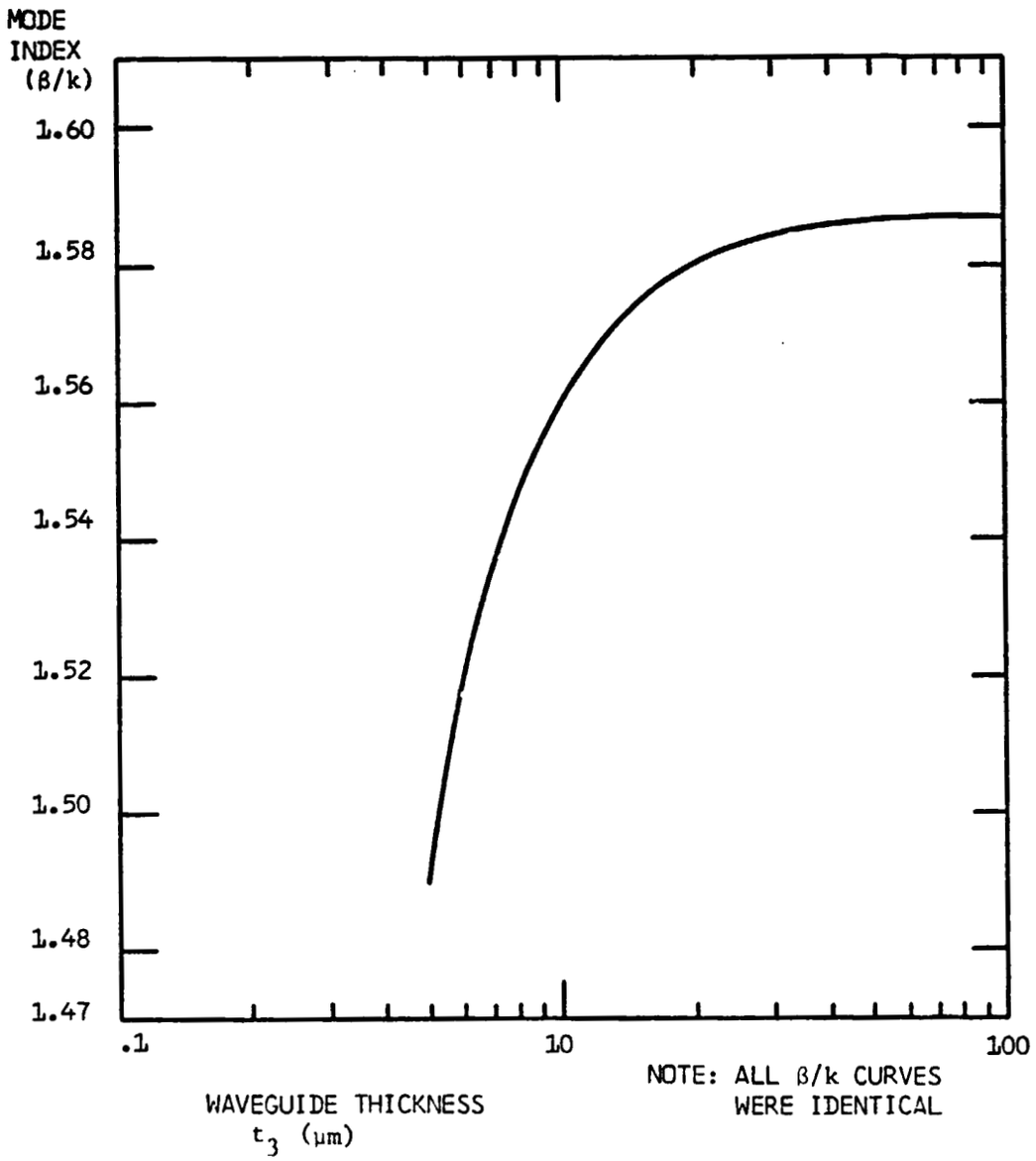

FIGURE 14. VARIATION OF ATTENUATION WITH Ga As CLADDING THICKNESS FOR THE TE_o MODE (t_3 = 1.0 um)

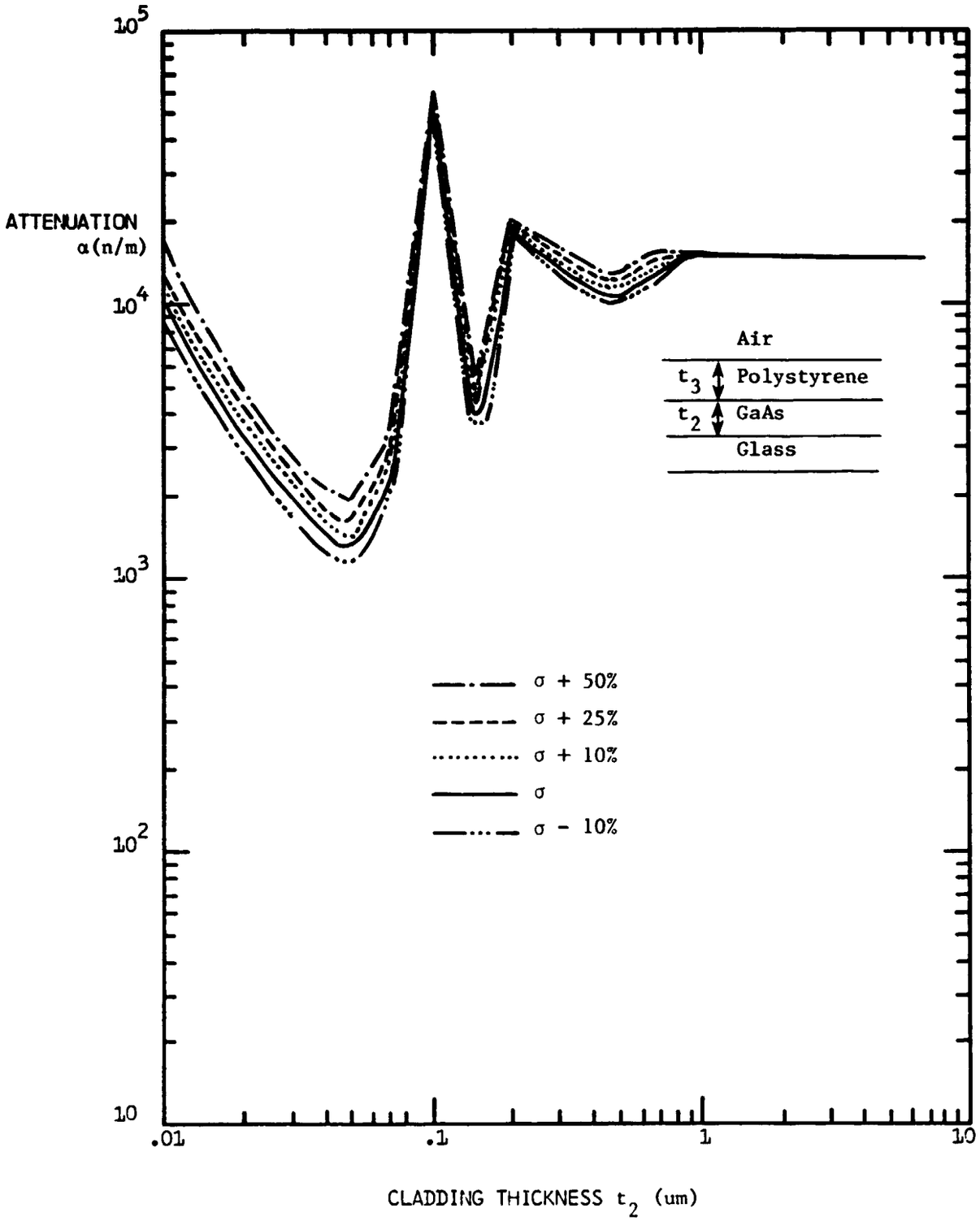

FIGURE 15. MODE INDEX VARIATION WITH GaAs CLADDING THICKNESS FOR THE TE_o MODE (t_3 = 1.0 μm)

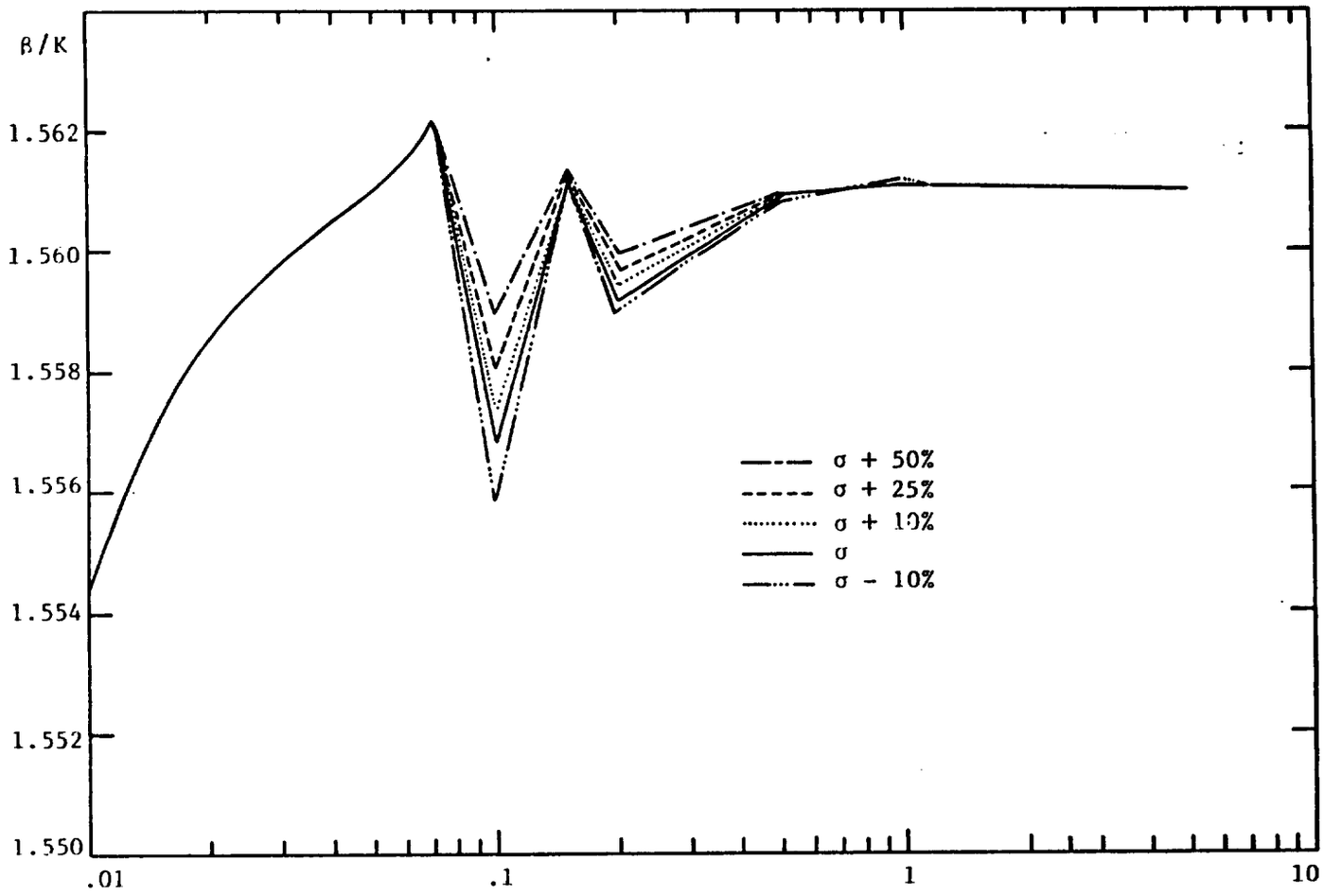

oscillation had never been observed before so it raised a number of questions about possible errors in the computer program.

If the predicted results are correct, then this could be used as a phase modulator since the change is mode index (.0022) at t_2 = .1 μm is large for a 50% change in conductivity. This mode index change would be equivalent to a 125 degree phase shift over a distance of 0.1mm, which is sufficient to make it applicable as a phase modulator. Addition calculations were run for the TM_o mode which exhibited similar characteristics to that of the TE_o mode.

At first we felt that the oscillations in attenuation and phase constant might be produced by discontinuities in the tangent function. In some of our previous calculations we had observed a jump in a normally smooth index curve. This was ultimately attributed to a discontinuity in the tangent function causing the computer program to calculate values of mode index and attenuation for a higher or lower order propagating mode. Our first step in verifying the results was then to fill in intermediate points between those we had calculated to make sure the curve was continuous.

Figures 16 and 17 show the variation with t_2 for a fixed conductivity (normal value) after additional points were calculated. Now the oscillation is even more pronounced and there seems to be a discontinuity in the mode index curve at 0.09 um. At thicknesses greater than 0.1 um the curve appears to be continuous. There are several other interesting things to note about the curves in Figures 16 and 17. First we note that the period of oscillation is about 0.1 μm. Since there was no waveguide dimension equal to 0.1 μm and the wavelength (632.8 nm) does not appear to be related to the oscillation period, there was no ready

FIGURE 16. GaAs/GLASS-CLAD WAVEGUIDE ATTENUATION vs t_2 (TE_o MODE, NORMAL CONDUCTIVITY)

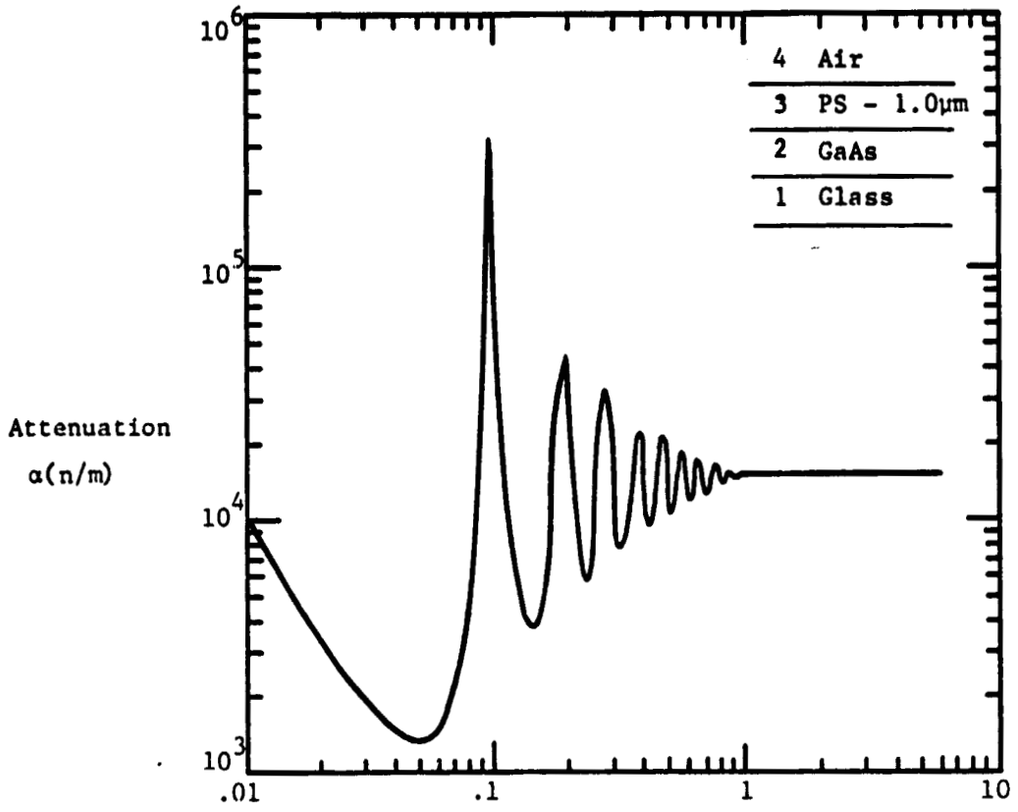

FIGURE 17. GaAs/GLASS-CLAD WAVEGUIDE β/K vs t_2 (TE_o MODE, NORMAL CONDUCTIVITY)

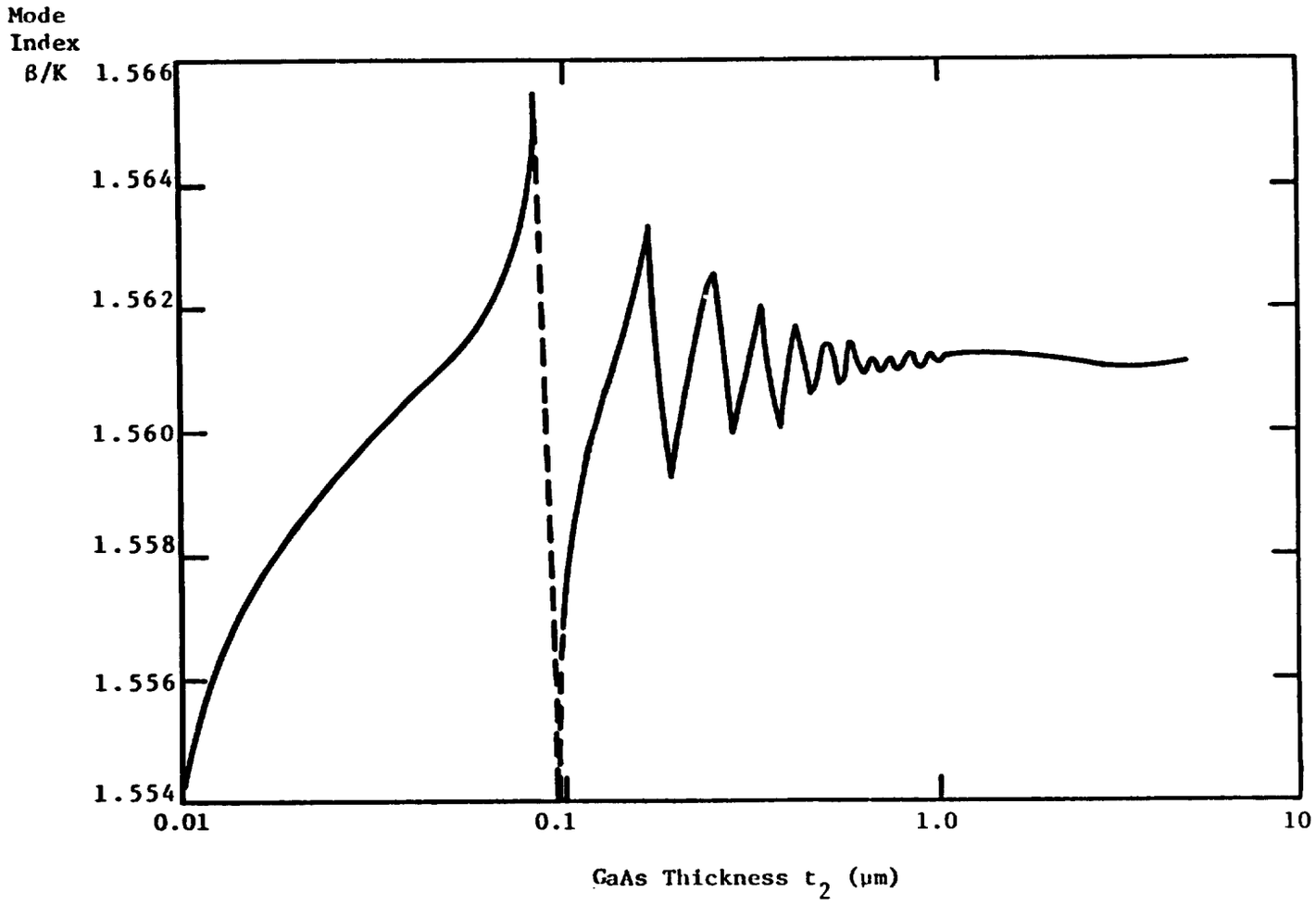

explanation for this observed oscillation. The second point to note is that the amplitude builds up almost exponentially as the thickness decreases.

Again we were somewhat surprised by the results so we chose a new waveguide thickness (t_3 = 0.8 um) and we also moved the GaAs cladding to the top of the waveguide. It was felt that these changes would eliminate any possibility of having accidently chosen a set of waveguide parameters which presented computational problems to the program because of discontinuities or extremely small arguments. Figures 18 and 19 show that the change in t_3 and the location of the cladding did change the amplitude of the oscillation slightly, but in general the characteristics of the attenuation and mode index curves were the same as before.

C. Material Selection

The only parameter which remained to be varied was the cladding material. From previous experience with waveguides of this type, we knew that small changes in the refractive index of the substrate, the waveguide or the material in region 4 would produce very slight changes in the characteristics, so these three parameter were not varied. It was decided to look at the three most common semiconductors and see what effect the material permittivity had on the results. Since GaAs had already been investigated, silicon and germanium were used as claddings. The complex permittivities and refractive indices are shown in Table I which follows.

FIGURE 18. GaAs/AIR-CLAD WAVEGUIDE ATTENUATION vs t_2 (TE_o MODE, NORMAL CONDUCTIVITY; t_3 = 0.8 μm)

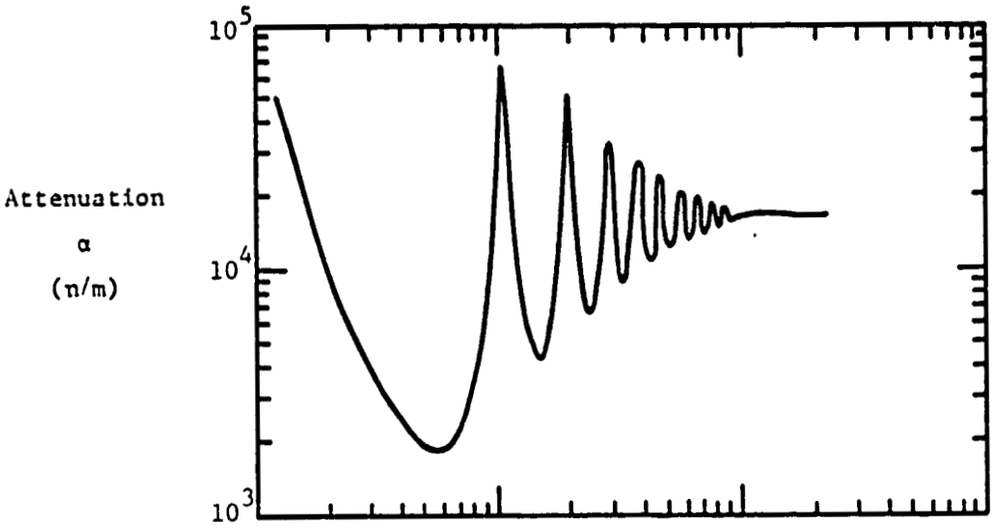

FIGURE 19. GaAs/AIR CLAD WAVEGUIDE

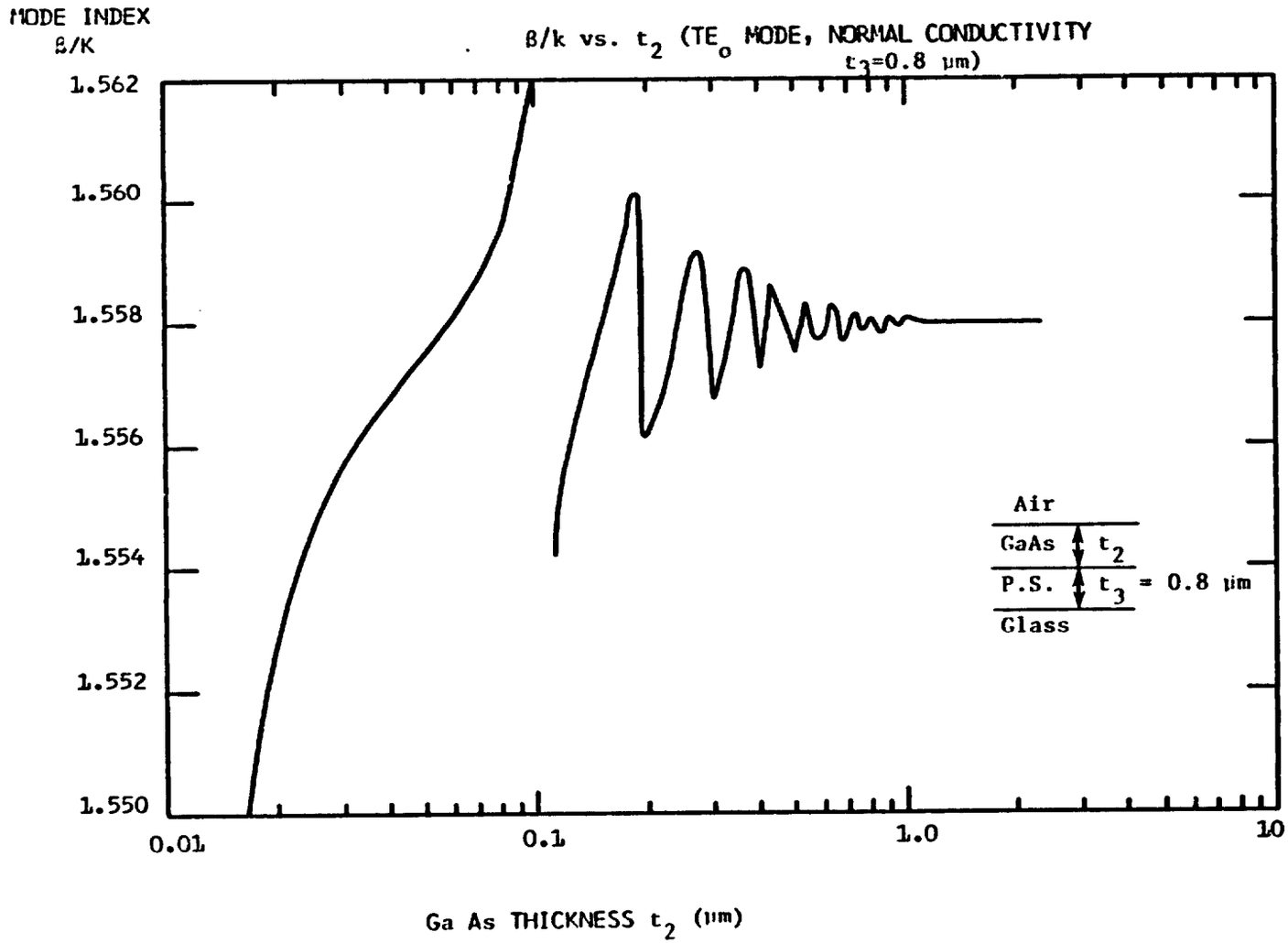

Table I

Semiconductor Parameters at λ = 632.8 nm

Material	Permittivity		Refractive Index	
	ε'	ε''	n	k
GaAs	14.3	1.21	3.79	0.16
Silicon*	16.76	1.75	4.1	0.213
Germanium*	14.43	19.54	4.4	2.22

*values for amorphous thin films

Note that the relative magnitudes of the real and imaginary parts of the complex permittivity of gallium arsenide and silicon are the same. Germanium, however, has a considerably higher imaginary part (conductivity) than either silicon of gallium arsenide. If material conductivity has any effect on the characteristics observed it should be evident in germanium. Figures 20, 21, 22 and 23 show the results for silicon and germanium. As might be expected, silicon exhibits characteristics nearly identical to those of GaAs. Germanium shows almost none of the oscillations which were characteristics of GaAs.

These results are not as surprising as originally thought in light of similar predictions in reference 14. In Figure 6.15 (Ref. 14) the author calculates the expected phase change on reflection at an air-film surface. The surface considered by the author is a thin film of material with n = 2 and k varying. The value of k at λ = 578 nm varied from 0 to 2 and the thickness of the material was varied from 0 to 140 nm. This material was on a glass substrate with refractive index of 1.5. For k very small the phase change was found to oscillate while for k large (k = 2) the phase changed very little until the thickness approached zero. Figure 24 is a sketch of the results obtained for the

FIGURE 20. SILICON/AIR CLAD GUIDE ATTENUATION vs t_2 (TE_o MODE, NORMAL CONDUCTIVITY)

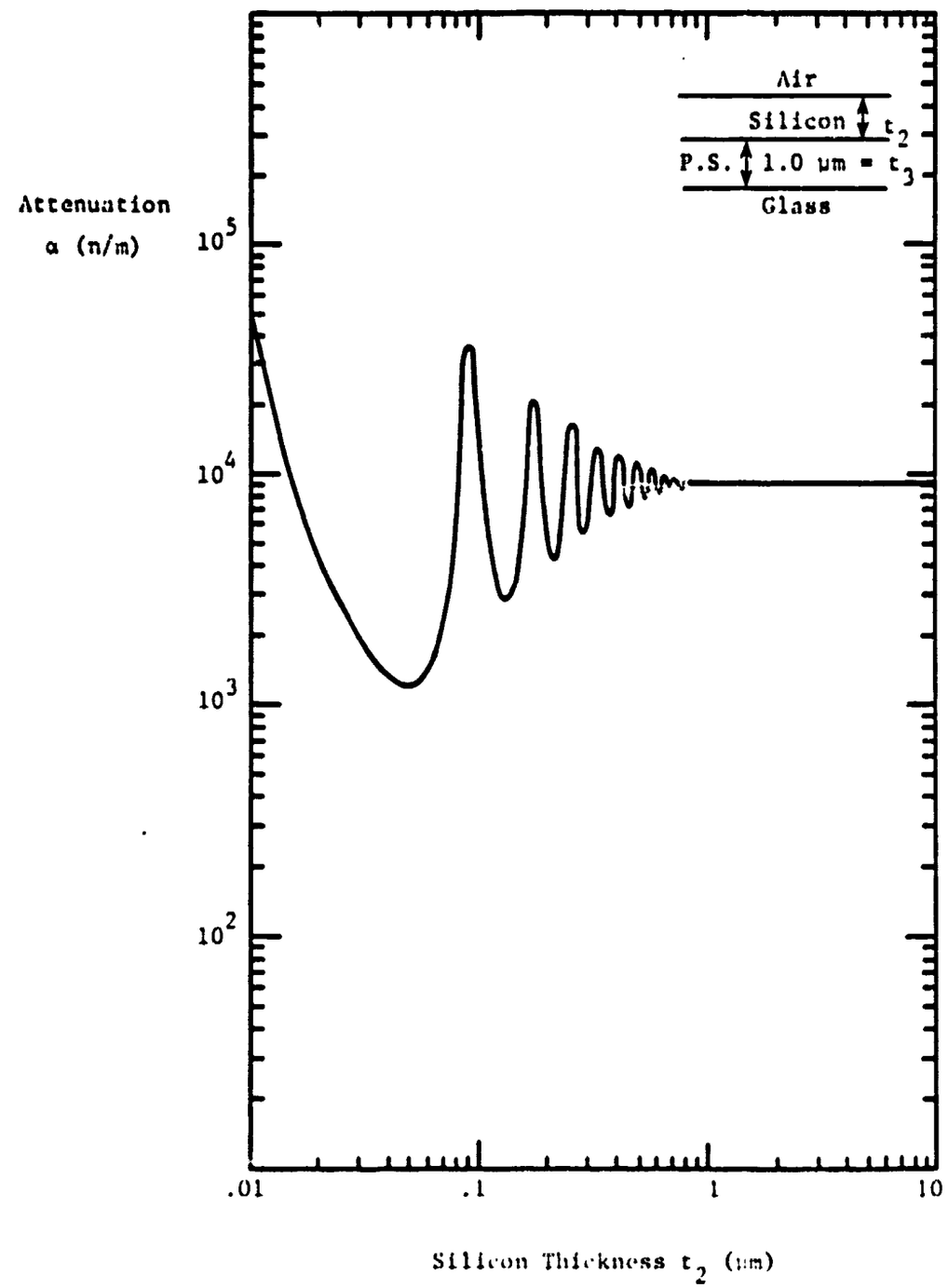

FIGURE 21. SILICON/AIR CLAD GUIDE β/K vs t_2 (TE_o MODE, NORMAL CONDUCTIVITY)

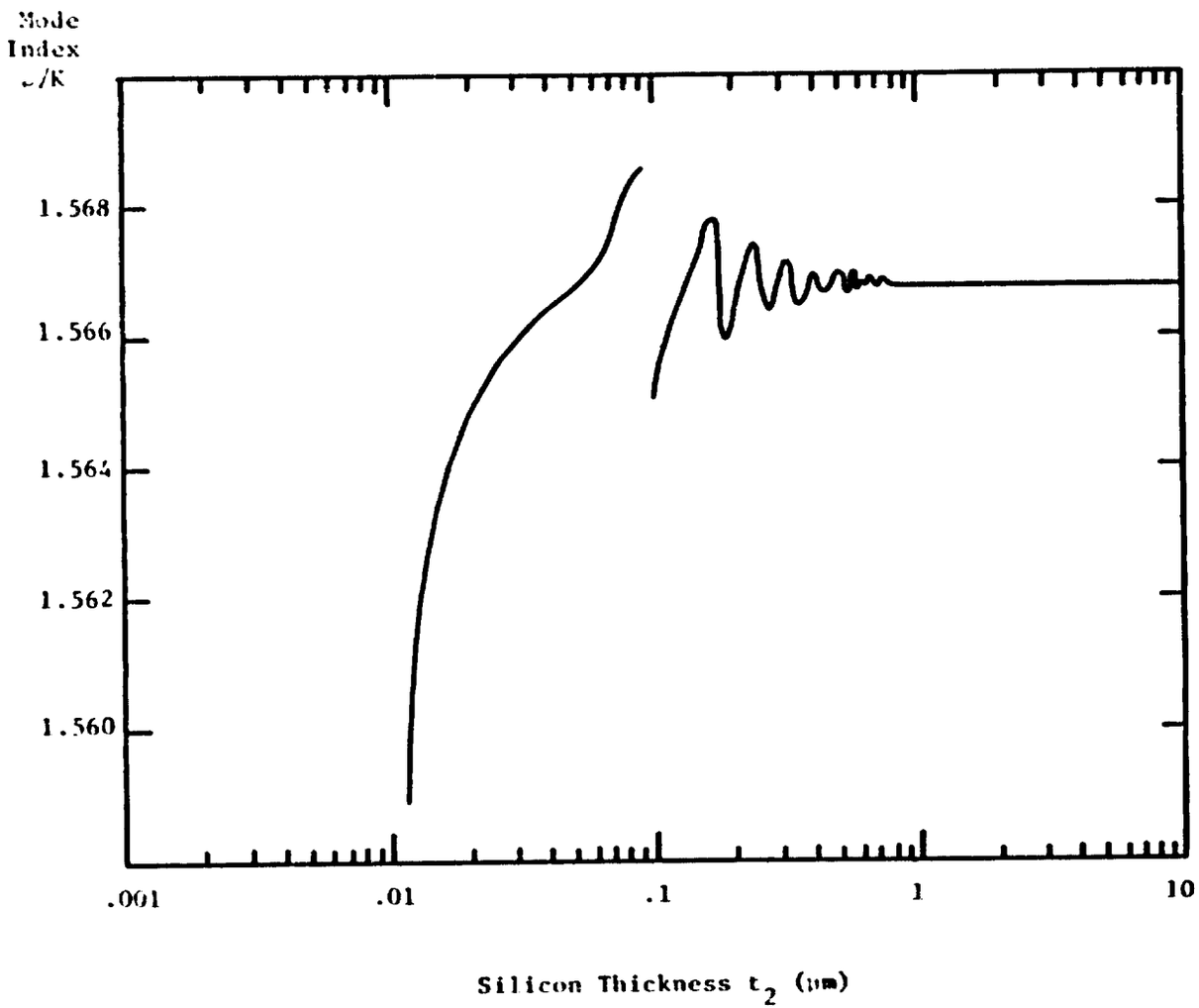

FIGURE 22. GERMANIUM/AIR CLAD GUIDE ATTENUATION Vs t_2
(TE_o MODE, NORMAL CONDUCTIVITY)

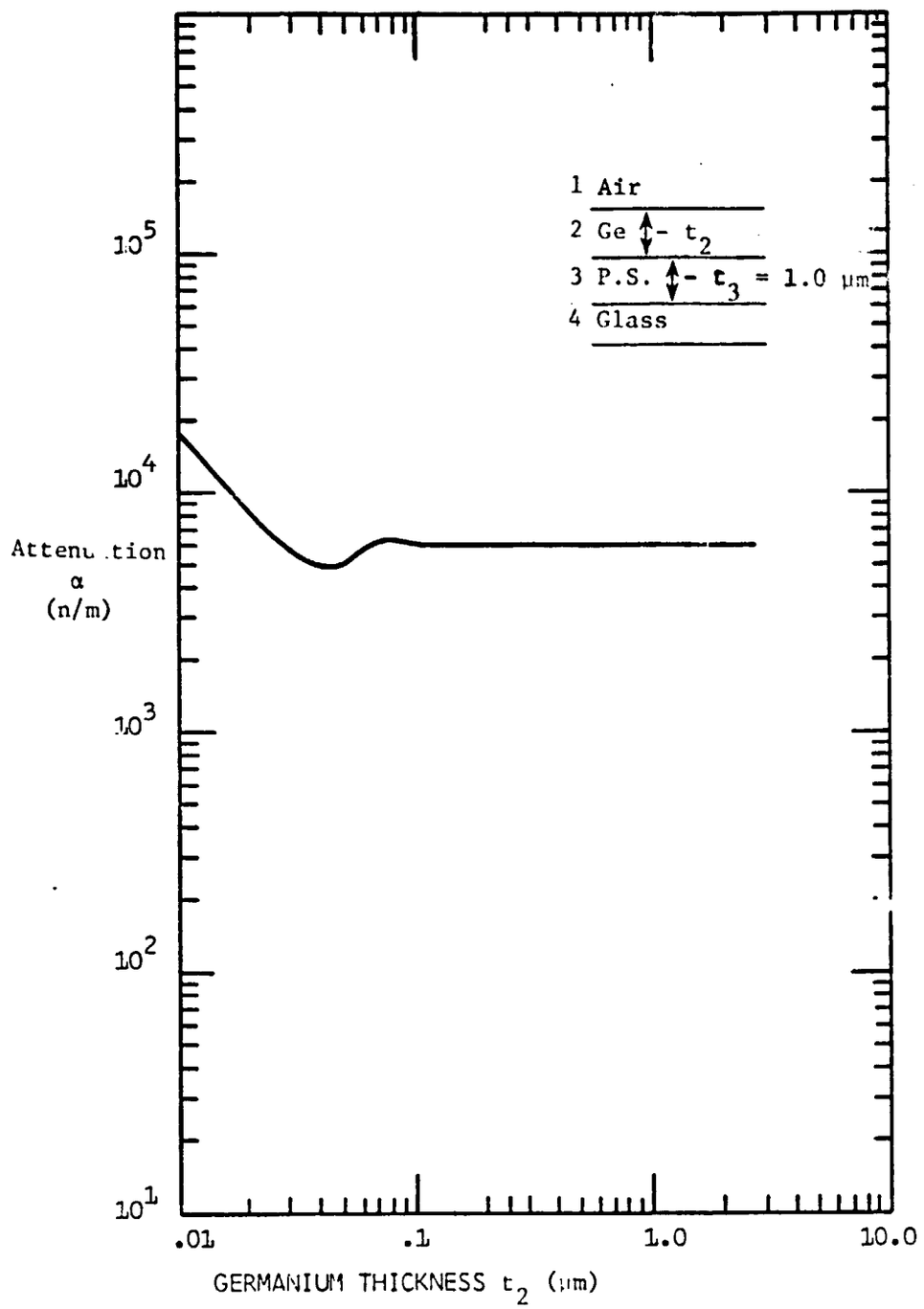

FIGURE 23. GERMANIUM/AIR CLAD GUIDE, β/K vs t_2
(TE MODE; NORMAL CONDUCTIVITY)

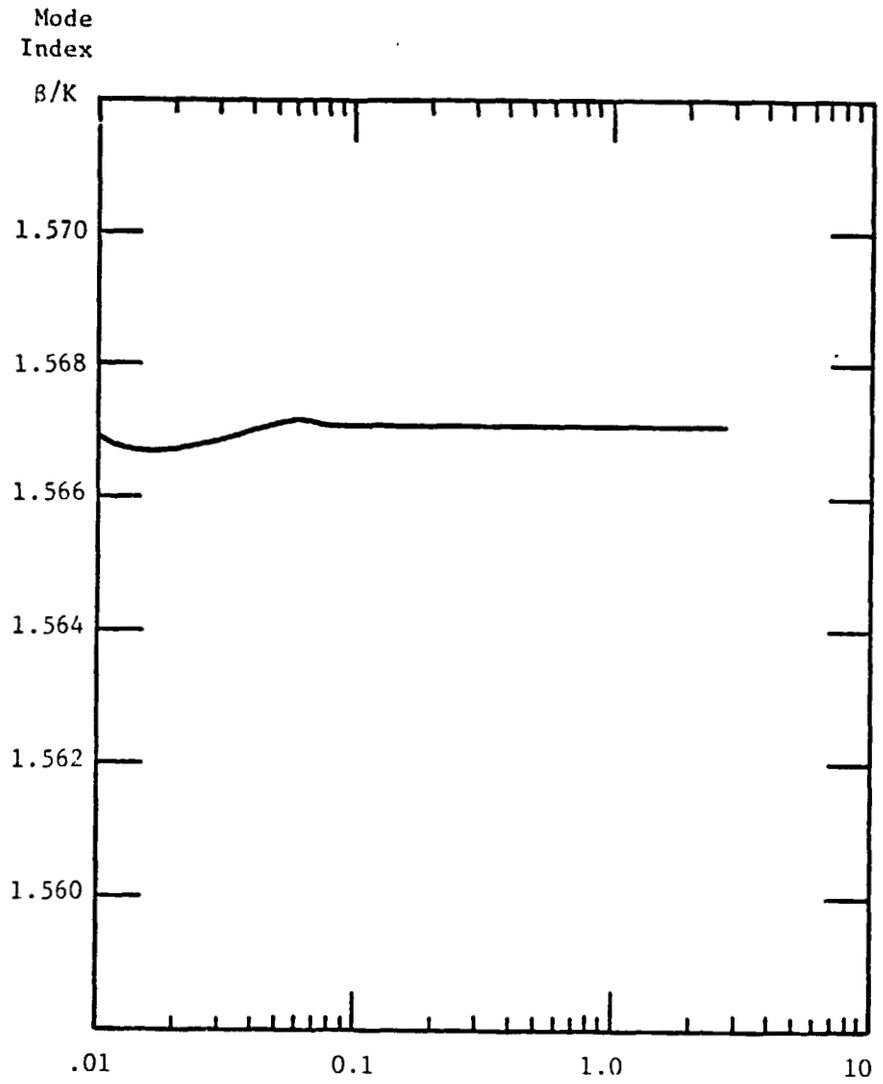

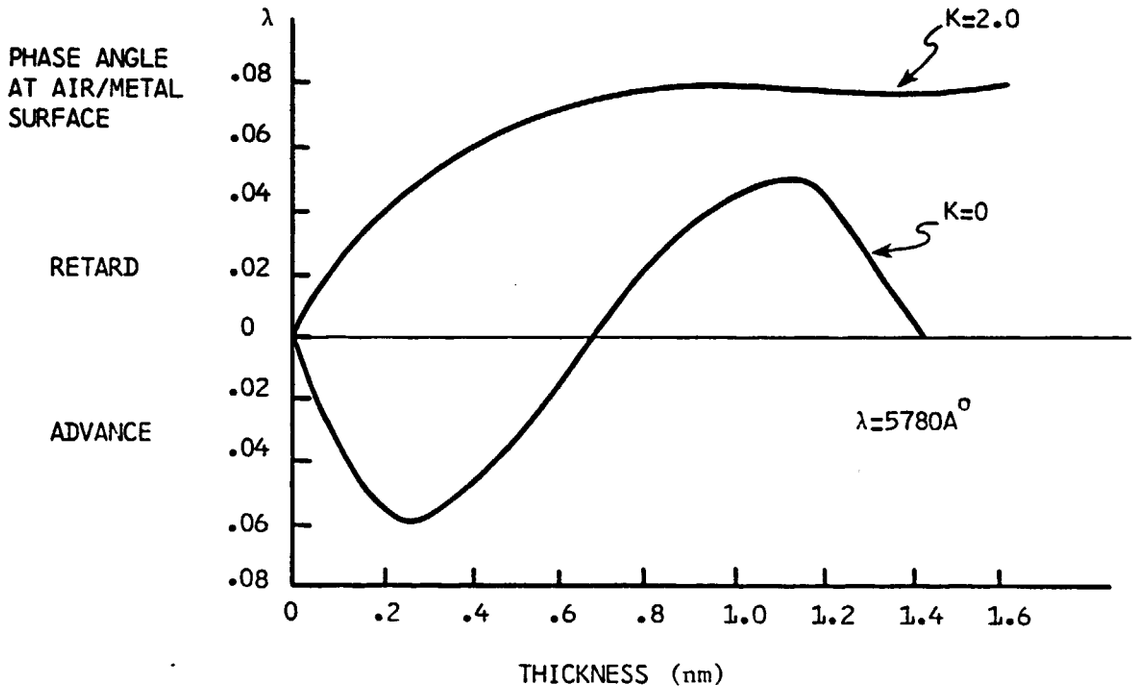

FIGURE 24. PHASE CHANGE (AT AIR SURFACE) VS. THICKNESS OF A FILM WITH N=2 AND K=0 AND 2. BASED ON REF. 14.

extreme values of k in reference 14. Note that for k = 0 the period of oscillation of the phase change curve is nearly one-tenth micrometer as we have observed in our calculated curves. Unfortunately the author does not discuss the oscillation between phase advance and retardation but goes into the problems of measuring such for experimental films.

D. Conclusions

In this section we have shown that by proper choice of the photoconductive layer thickness we can maximize the induced phase chage in the wave propagating in the guided region for a given change in conductivity. Figure 25 shows the total attenuation suffered by a wave propagating over a length of modulating semiconductor. For a 2mm length modulation region a 4 neper (34.1 dB) change in attenuation occurs with a 50% change in conductivity. Unfortunately the overall attenuation of the device is large (100 dB).

Table 2 illustrates the phase shift expected in GaAs if the modulator was used as a phase modulator and the modulation length was taken as 1 mm. Obviously the modulator length could be reduced to 0.1 mm for phase modulation and still produce a detectable phase shift of 0.3 rad. for a 10% conductivity change in the worst case (TE_o, t_2 = 0.2 um). For this length modulation region the device should have less than 20 dB attenuation. Further work will be needed to optimize the phase modulator to reduce this inherent attenuation. For example, use of the higher order modes in the waveguide which suffer less attenuations and also use of silicon will likely produce a lower loss modulator.

Previous work [15] has shown that the inclusion of a thin dielectric buffer layer between a dielectric waveguide and a thick metal cladding reduces the attenuation significantly while having very little

FIGURE 25. ATTENUATION VS. MODULATION LENGTH AS A FUNCTION OF CONDUCTIVITY (TE_o MODE, t_2= 0.15 μm, t_3= 1.0 μm) ---------> GaAs CLADDING)

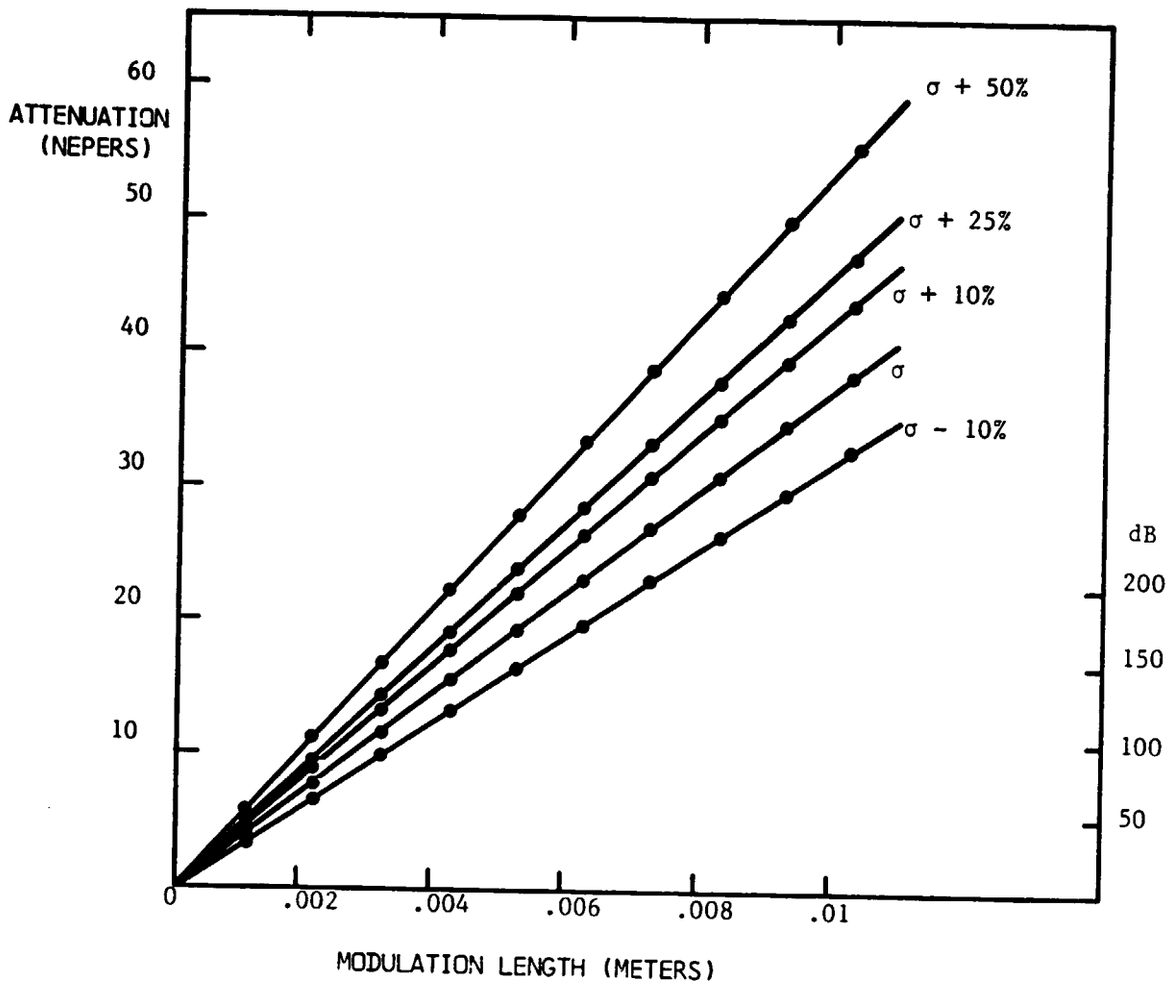

TABLE 2

Phase Shift at Points of Maximum β/K Variation
(GaAs, t_3 = 0.8 μm)

Mode	T2	Conductivity (σ)	β (x 10^7)	% difference	Δ φ (at 1 mn)
TE_o	.2μm	σ	1.53303	-----	-----
		σ - 15%	1.53253	.033%	1.6 π
		σ + 10%	1.53332	.019%	0.9 π
		σ + 15%	1.53347	.029%	1.4 π
		σ + 25%	1.53375	.047%	2.3 π
	.1μm	σ	1.52788	-----	-----
		σ - 15%	1.52645	.094%	4.6 π
		σ + 10%	1.52883	.062%	3.0 π
		σ + 15%	1.52928	.092%	4.5 π
		σ + 25%	1.53014	.148%	7.2 π
TM_o	.4μm	σ	1.51491	-----	-----
		σ + 10%	1.51565	.049%	2.4 π
		σ + 25%	1.51720	.151%	7.3 π
		σ + 50%	1.52264	.510%	24.6 π
	.5μm	σ	1.52485	-----	-----
		σ + 10%	1.52630	.095%	4.6 π
		σ + 25%	1.52810	.213%	10.3 π
		σ + 50%	1.53213	.477%	23.2 π
TE_1	.2μm	σ	1.39568	-----	-----
		σ + 10%	1.39617	.035%	1.6 π
		σ + 25%	1.39702	.096%	4.3 π
		σ + 50%	1.39864	.212%	9.4 π
TM_1	.1μm	σ	1.45774	-----	-----
		σ + 10%	1.45617	.108%	5.0 π
		σ + 25%	1.45447	.224%	10.4 π
		σ + 50%	1.45321	.311%	14.4 π
	.7μm	σ	1.43428	-----	-----
		σ + 10%	1.43237	.133%	6.1 π
		σ + 25%	1.42925	.351%	16.0 π
		σ + 50%	1.42253	.819%	37.4 π

effect on the mode index of the TE_o mode. Such techniques will require modification of the existing computer program and will be investigated during the next reporting period.

One additional problem has yet to be addressed before evaluating the feasibility of the phase modulator. The assumed conductivity changes must be produced by the available incident photons; that is, the photon conversion to hole-electron pairs must be efficient enough to produce the desired conductivity changes. Referring to equation (3), we see that the percent conductivity change will be a function of the dc conductivity (σ_o), the photon generated hole-electron pairs and the mobilities of holes and electrons. Values for these parameters must be found for thin films likely to used in a modulator.

Silicon was chosen as a good candidate for a modulator film since it can be easily deposited as a thin amorphous film on a glass substrate. GaAs is much more difficult to deposit in thin layers on glass and the optical properties of such films are not known.

Since the electrical characteristics of amorphous silicon vary widely with methods of desposition, temperature and pressures, it has also been necessary to estimate the needed parameters from published data and carry out a worst case calculation of percentage conductivity change.

Mobilities are complicated functions of frequency, temperature and interatomic spacing; however, one source [39] has measured the mobilities to be less than 5 $cm^2\ v^{-1}\ sec^{-1}$. Steady state (dc) resistivity was found to vary from 10^3 to 10^5 ohm - cm at 300 K and more recently resistivities as high as 10^8 ohm-cm were produced by silane deposited films [40]. The worst case approximation for resistivity (10^3 ohm-cm)

produces 1.5 x 10^{14} cm^{-3} thermally generated electron-hole pairs at 300K. For a small volume of material likely to be used in a modulator (2 x 10^{-5} cm x 10^{-2} cm x 1 cm), there are 3 x 10^{7} electron-hole pairs thermally generated in the steady-state. If we assume the number of incident photons is 10^{14}/sec and 75% are reflected at the surface (anti-reflection coating could decrease this reflectivity) as discussed before, then the number electron-hole pairs can be calculated knowing the number of photons absorbed and the quantum efficiency. The attenuation coefficient of amorphous silicon was measured as $\alpha = 4.23\ (\mu m)^{-1}$ at λ = 0.6328 μm giving 2 x 10^{13} photon/sec absorbed by the cladding material. With an estimated quantum efficiency of 10% and electron-hole lifetimes of 10^{-6} sec (this varies from 10^{-3} to 10^{-6} sec),[41] this produces a minimum of 2 x 10^{6} electron-hole pairs which increases the conductivity by 6.7%. Thus variations of 50% in the light intensity would only produce 3.3% change in the conductivity.

This worst case analysis simply indicates that the device is feasible even under those conditions. Using measurements for better amorphous silicon films[40] gives even more encouraging results. In this reference films of 1 μm thickness having resistivities of 10^{8} ohm - cm produced a 7% change in conductivity for a 10% change in incident light level (light level was taken at 10^{-2} AM1). Thus we see that it is likely that we can deposit films with better electrical characteristics than those used in the worst case analysis.

Based on the above analysis and the measured data on amorphous semiconductors we conclude that the modulator is feasible and a set of experiments should be performed to verify the calculated feasibility. These experiments are described in the next section.

IV. FABRICATION OF ION EXCHANGED WAVEGUIDES

Since the silicon films forming the modulator must be vacuum deposited, often at substrate temperatures greater than 200 ^{o}C, the polystyrene waveguides previously used were unsatisfactory in this environment. Ion exchanged waveguides were selected as the optimum type guide for development of the modulator. High quality waveguides can be diffused into soda-lime microscope slides quickly and easily using the technique described in the following paragraphs.

Several authors have reported on the fabrication and characteristics of ion exchanged optical waveguides (42-46). This technique involves the diffusion of silver ions into soda-lime glass and the subsequent replacement of sodium ions which diffuse out of the glass. The index of refraction of the glass is raised; thereby forming a waveguide on the surface of the glass. Guides supporting from one to ten guided modes have been fabricated by varying diffusion times from 30 seconds up to 30 minutes.

Pure silver nitrate was melted in a covered stainless steel beaker and clean soda lime glass slides were placed in a covered pyrex dish on the hot plate. A stainless steel bracket for holding the slides and a thermocouple temperature probe were placed in the silver nitrate melt and the system was allowed to thermally equilabrate at 247^{o}C. The bracket was removed from the melt, a preheated slide was placed in it and the assembly returned to the melt for 30 minutes. The slide was removed, allowed to cool and rinsed in de-ionized water. All the guides formed with the preceeding procedure were lossy, had very high scattering, were discolored and had a precipitate on the surface. There were 22 to 27 supported propagating modes. It was noted that the nitrate

melt had also been contaminated by a brass temperature probe used for measuring the temperature of the melt.

A dilute melt of ratio 1 mole of the silver nitrate to 20 moles of sodium nitrate was tried next (43). The stainless steel was pickled[1] and guides were formed in the new solution at 245°C for diffusion times of 30 minutes. The guides were clear, low-loss, had no surface deposits and supported ten guided modes. The brass temperature probe had been electroplated with gold to prevent contamination but the silver nitrate solution transferred the gold onto the stainless steel and plated the probe with silver. On the next trial the probe was plated with silver and it was found that the silver nitrate still etched the probe. No solution to this etching problem has been found at this time.

The controlable parameters in this fabrication procedure are temperature, diffusion time and the mole fraction of the silver nitrate melt. The melt mole fraction was not changed in any of our tests since low-loss high quality guides were formed with the 1 to 20 ratio. Diffusion times were varied from 30 seconds to 30 minutes and diffusion temperatures of 215°C, 245°C, and 260°C were investigated.

The effect of the diffusion temperature was to increase the rate of silver/sodium ion exchange with increased temperature. Since the purpose of this investigation is to fabricate quality waveguides with repeatability, the temperature was held just above the melting point of the melt to keep the ion exchange process as slow as possible in order to determine diffusion times.

[1]Pickling is used to clean the stainless steel. The solution used is 1 part HF, 8 parts nitric acid, 4 parts sulfuric acid, and 51 parts water.

Single mode optical waveguides were formed in 30 seconds when the diffusion temperature was held at 215°C. The only scattering observed in these guides is at the surface of the glass slide and this can be eliminated by using polished, optically flat microscope slides. Table 3 is a tabulation of the number of propagating modes the fabricated waveguide supports with diffusion time as a parameter.

Table 3

number of modes	diffusion time
9	30 min.
7	15 min.
5	10 min.
4	5 min.
2	2 min.
1	45 sec.
1	30 sec.

The guides were all fabricated with a .05 mole fraction silver nitrate/sodium nitrate melt and at 215°C $\pm$ 4°C.

This very simple fabrication procedure produces repeatable waveguides of very low loss. In some of the references, (42,43,44) the authors reported the guides were buried into the glass slide. We observed no burying of the guide and verified this by scratching the surface of the guide which stopped the propagating wave. Over a period of four months, no noticible breakdown of the guides has been observed.

Although these waveguides have not been completely characterized at this time to relate temperature to number of propagating modes, reliable guides with attenuations < 1.0 dB/m have been repeatedly produced. The waveguides are also stable over a period of four months with no change in attenuation or number of propagating modes noted. The only problem we have encountered has been in accurately measuring the melt temperature without significant contamination of the melt.

V. EXPERIMENTAL DEVICES

Based on the calculations in section 3 several devices are currently being constructed to verify the predicted attenuation variation with cladding thickness. Such devices will serve to verify the calculations and prove that the magnitude of the effect is large enough for use as a modulator.

Discussions with several people working with amorphous semiconductors indicate potential variation in the optical properties of these amorphous films with deposition method and temperature. Thus values of refractive index and loss coefficients used in our calculations may not be accurate for real films. After initial investigation of the two principal methods of deposition of amorphous silicon (CVD and e-beam evaporation) it was decided to use the e-beam technique because of better reproducibility in optical constant. Use is being made of the e-beam system of Cornell University, Materials Science Department, for our initial films.

Films thickness have been selected based on the predicted attenuation and phase variations in section 3. Figure 26 shows the predicted percentage change in attenuation as a function of silicon thickness. Guides are being fabricated with a silicon thickness of 0.18 micrometers to attempt to achieve the maximum percentage variation as predicted. Obviously, if the optical parameters of the films vary significantly from those used in our calculations, we may find the device is at a minimum change point rather than the maximum. If this turns out to be the case the device will then be useful as a phase modulator since Figure 27 shows the minimum attenuation produces the maximum phase shift.

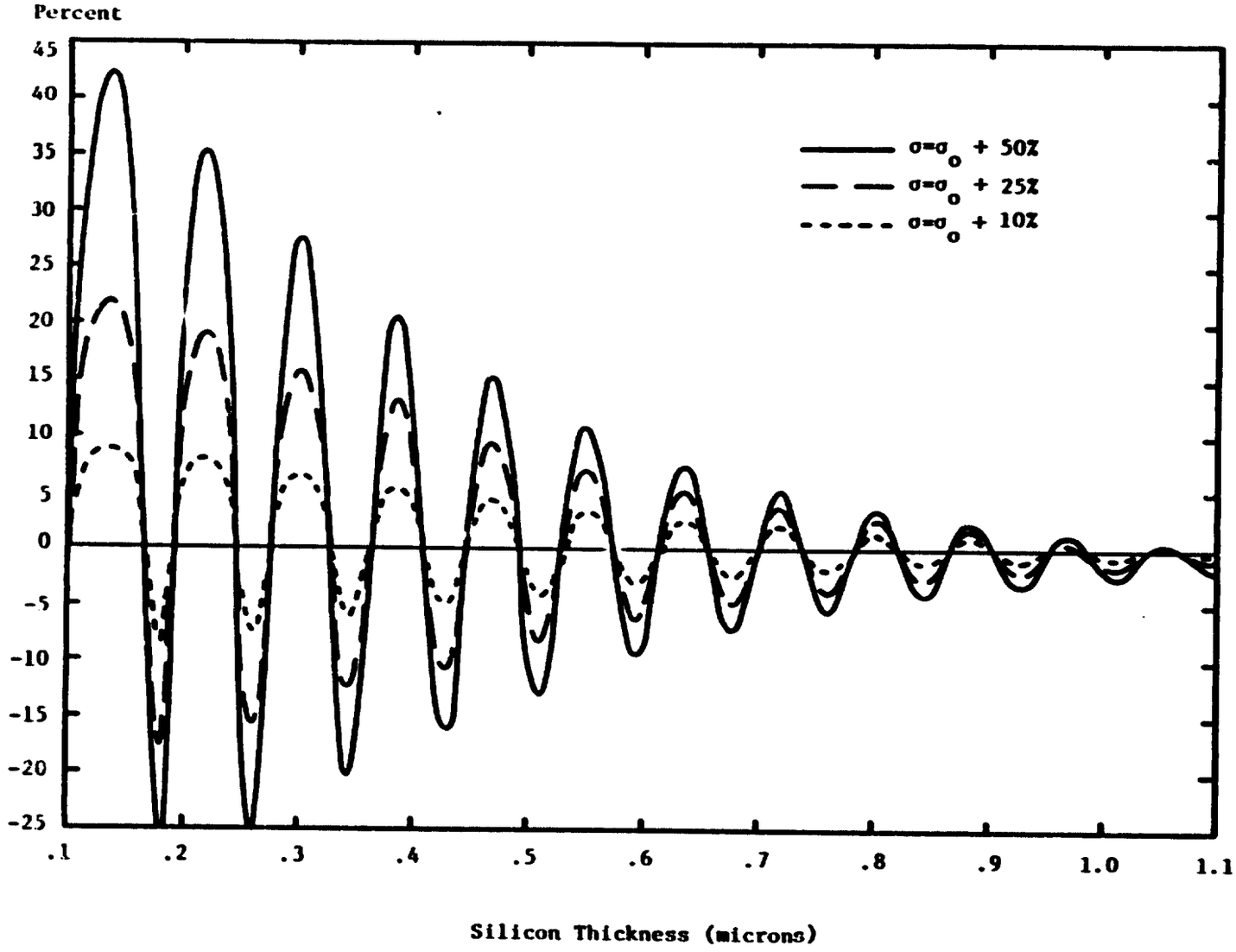

Figure 26. Calculated Percent Change in Attenuation Over Attenuation Calculated at 10 Micrometers Thickness for the TE_o Mode (t_3 = 1.0 μm).

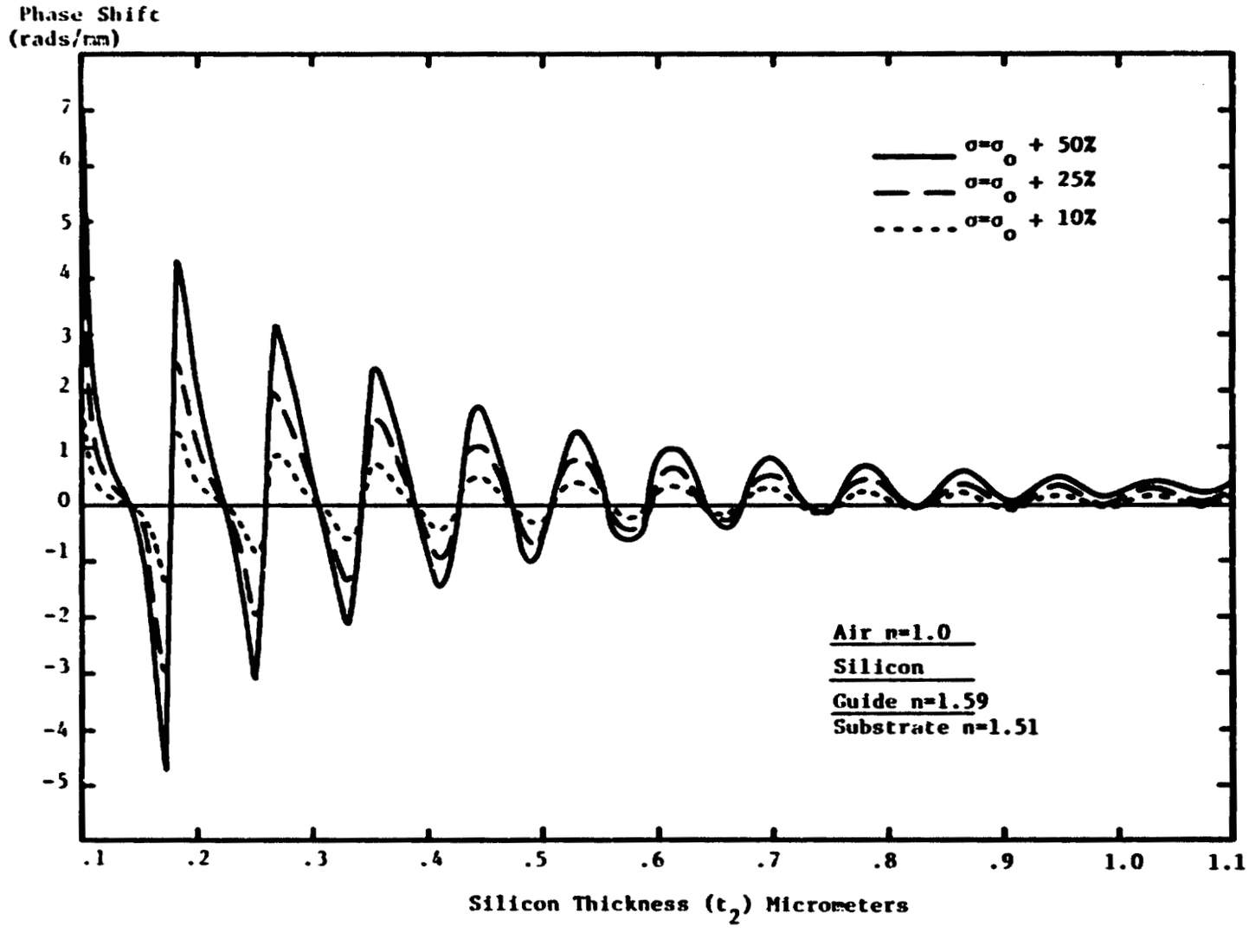

Figure 27. Calculated Relative Phase Shift Compared to that Calculated for a Silicon Thickness of 10 micrometers.

A wedge shaped film varying in thickness from 0.1 to 1.0 micrometers has been studied and an experimental film is being attempted. Such a film would allow measurement of all variations shown in Figure 26 or 27. After the films have been deposited a number of experiments will be attempted as discussed below.

A. Verification Experiments

There are three experiments which can be used to verify the predictions and confirm that the magnitude of the effect is large enough for use in a modulator. Figure 28 shows the experimental device to be used in the first two experiments. A silicon wedge varying in thickness from 0.1μm to 1 μm and 0.1 mm wide will be vacuum deposited on an optical waveguide. The use of the wedge shaped silicon layer should allow us to observe the variation in attenuation when a wide beam is coupled into the guide. If the propagating beam is wide enough it should cover several attenuation oscillations and appear as a sinusodial fluctuation in the intensity across the transverse waveguide direction. This would be easily visible and measureable with a detector.

The second experiment will make use of the same waveguide and wedge as shown in Figure 28. The silicon wedge will be illuminated with an incoherent light source and the signal on the output side of the wedge will be measured as a function of the coherent light intensity.

If both of these experiments are successful, the phase modulation experiment will be attempted. The waveguide for the phase modulation experiment is shown in Figure 29. For this test a thin film of silicon would be deposited half-way across the waveguide. A beam coupled into the waveguide would pass half under the silicon region and half in the normal waveguide. The energy coupled out should form an interference

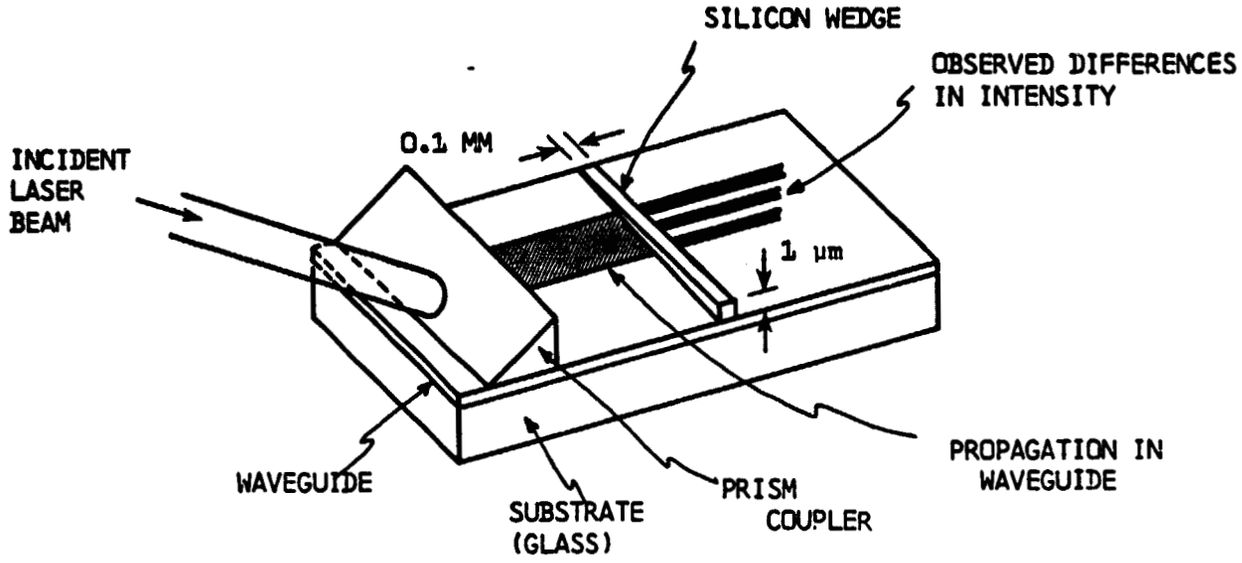

FIGURE 28. PROPOSED EXPERIMENTAL DEVICE FOR VERIFICATION OF OSCILLATIONS IN INTENSITY.

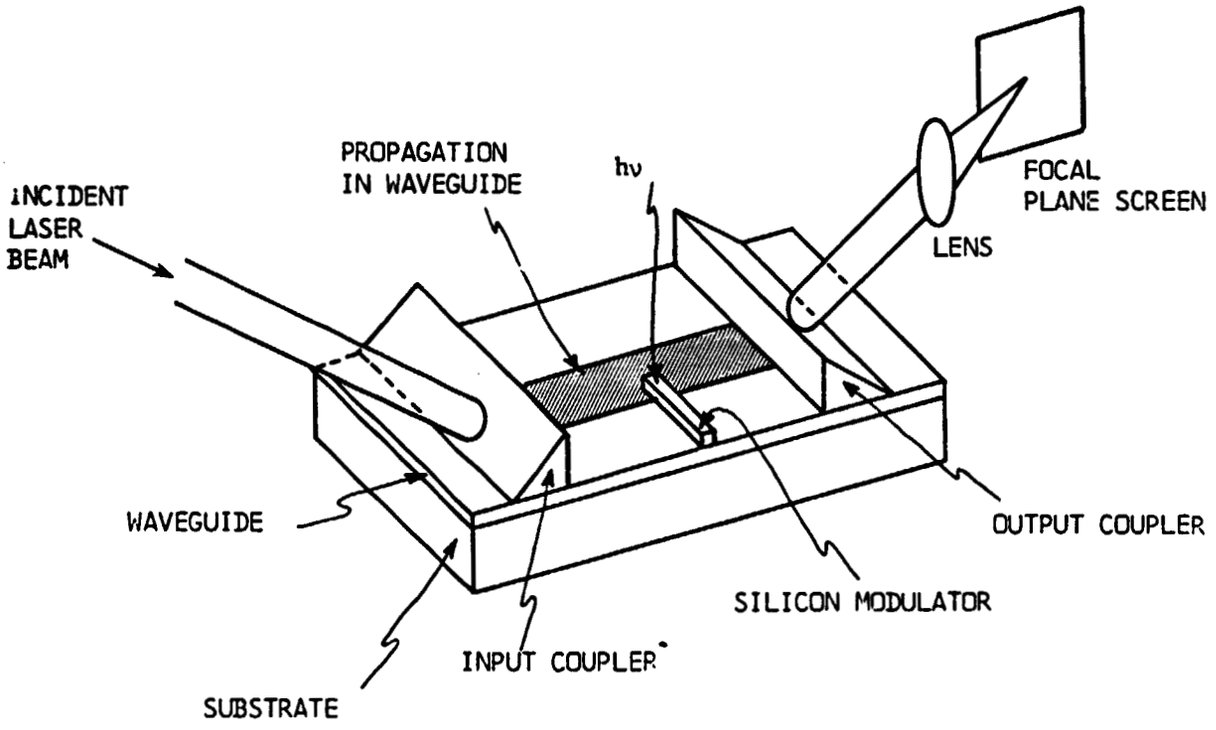

FIGURE 29. PROPOSED PHASE MODULATION EXPERIMENT.

pattern on the focal plane screen. Incident light on the silicon film should then produce a modulation of the fringe pattern on the screen thus verifying the phase modulation concept.

These experiments will depend on the successful deposition of thin amorphous silicon films in the configurations described above. Preliminary results with the Cornell e-beam evaporation system indicate the proposed films depositions are feasible so that experimental results should be forthcoming. We should note that while gallium arsenide was initially proposed for the modulator, vacuum deposition of thin films of GaAs is more difficult than silicon films, so all experiments will use silicon films.

B. The Phase Modulator

If the three experiments discussed above prove successful the next step will be to optimize the design of the modulator. This will involve decreasing the large attenuation predicted for the devices discussed above. Investigations of the effect of a buffer layer between the waveguide and the semiconductor are currently in progress. Waveguide, buffer layer and semiconductor materials and thicknesses will have to be seleced to optimize the modulation while minimizing the attenuation. New calculations will have to be made with this buffer layer on the ion exchanged waveguides rather than the polystyrene waveguides used in the current calculations.

Development of the phase modulator to its ultimate potential will require considerably more time and support than has been available in this preliminary grant. Effort is continuing under the follow-on grant to verify the concept.

REFERENCES

1. C.M. Verber, D.W. Vahey, V.E. Wood, R.P. Kenan and N.F. Hartman, "Feasibility Investigation of Integrated Optics Fourier Transform Devices," NASA Contractor Report July 1977, NASA CR2869.

2. V.E. Wood and C.M. Verber, "Study of Methods for Direct Optical Circuits," Final report, NASA Contract No. NAS115315, Battelle Colombus Laboratories, (Draft, April 1979).

3. W.L. Wolfe, ed., Handbook of Military Infrared Technology, Offices of Naval Research, Washington, D.C., 1965.

4. N.S. Kapany and J.J. Burke, Optical Waveguides, Academic Press, New York, 1972.

5. I.P. Kaminow, W.L. Mammel, and H.P. Weber, "Metal-clad optical waveguides: Analytical and experimental study," Appl. Opt., Vol. 13, pp. 396-405, Feb. 1974.

6. J.W. Bandler and P.A. Macdonald, "Optimization of Microwave Networks by Razor Search," IEEE Trans. on Microwave Theory and Techniques, Vol. MTT-17, No. 8, 1969, pp. 552-562.

7. D.H. Auston, "Picosecond optoelectronic switching and gating in silicon," App. Phys. Lett., Vol. 26, No. 3, 1 Feb. 1975, pp.101-103.

8. O.S.F. Zucker, J.R. Long, V.L. Smith, D.J. Page and P.L. Hower, "Experimental demonstration of high-power fast-rise-time Vol. 29, No.4, 15 Aug. 1976, pp.261-263.

9. J.M. Proud, Jr. and S.L. Normon, "High-Frequency Waveform Generation Using Optoelectronic Switching in Silicon," IEEE Trans. on Microwave Theory and Techniques, Vol. MTT-26, No.3, March 1978, pp.137-140.

10. Industrial Research/Development Vol. 21, No. 6, June 1979 pp.69-70.

11. J.H. Perlstein, "'Organic Metals' The Intermolecular Migration of Aromaticity" Angeu. Chem. Int. Ed. Engl. 16, No. 8 Aug 1977, pp. 519-534.

12. J.H. Perlstein, J.A. Allan, L.C. Isett and G.A. Reynolds, "Chemistry of the Mixed - Valent Charge Transport Process: The Design of Organic Molecules for Organic Metals," Anals of the New York Academy of Science, Vol. 313, pp. 66-78, Sept. 29, 1978.

13. J.H. Perlstein, "Structure and Charge Generation in Low-Dimensional Organic-Molecular Self-Assemblies," a chapter in Electrical Conductivity in Polymers, to be published by Academic Press.

14. O.S. Heavens, Optical Properties of Thin Solid Films, Academic Press, Inc. New York, 1955, pp.170-172.

15. S.C. Rashleigh, Planar Metal-Clad Dielectric Optical Waveguides, Phd Thesis, University of Queensland, Brisbane Australia, May 1975, pp. 199-200.

16. M. Herbluin, S.Y. Wang, J.R. Whinney and T.K. Gustafson "An Integrated MOM Device with Invarient Frequency Response from DC Up to Optical Frequencies," Optical Communication Systems, Rpt. of a Grantee-User Meeting at Columbia University, New York City, pp. 49-53, June 6-7, 1977.

17. D.P. Siu and T.K. Gustafson, "Stimulated Emission of Surface Plasmons by Electron Tunneling in Metal-Barrier-Metal Structures," Appl. Phys. Lett. 32(8), 15 April 1978, pp. 500-502.

18. T.K. Gustafson, "Photo Excitations," Optical Communications Systems, Proceedings of NSF Grantee-User Meeting, Pittsburgh, Pa., June 57, 1978, pp.148-171.

19. W. Steinmann, "Optical Plasma Resonances in Solids," Physica Status Soldidi, Vol. 28, 1968, pp. 437-462.

20. P.M. Platzman and P.A. Wolff, Waves and Interactions in S olid State Plasmas, Academic Press, New York, 1973.

21. A. Otto, "Excitation by Light of $\omega+$ and $\omega-$ Surface Plasma Waves in Thin Metal Layers," Zeitschrift fur Physik, Vol. 219, 1969, pp. 227-233.

22. A.S. Barker, "Optical Measurements of Surface Plasmons in Gold," Physical Review B, Vol. 8, No. 12, 1973, pp. 5418-5426.

23. A. Otto, "Optical Excitation of Nonradiative Surface Plasma Waves," Physica Status Solidi, Vol, 42,1970, pp.K37-K39.

24. A. Otto, "Plasmaschwingungen gebundener Elecktronen: Der Characteristische Energieverlust von 3.6 eV in dunnel Silberfolien," Zeitschrift fur Physik, Vol. 185, 1965, pp. 232-262.

25. R.H. Ritchie, "Surface Plasmons in Solids," Surface Science, Vol. 34, 1973, pp. 1-19.

26. A. Otto, "Excitation of Nonradiative Surface Plasma Waves in Silver by the Method of Total Reflection," Zeitschrift fur Physik, 216, 398-410.

27. A. Otto, "Optical Excitation of Nonradiative Surface Plasma Waves," Phys. Stat. Sol 42, K37 (1970), short notes.

28. P.K. Tien and R.J. Martin, "Experiments on Light Waves in a Thin Tapered Film and a New Light-Wave Coupler," Applied Physics Letters, Vol. 18, May 1, 1971, pp. 398-401.

29. D. Marcuse and E.A.J. Marcatili, "Excitation of Waveguides for Integrated Optics with Laser Beams," Bell System Technical Journal, January 1971, pp. 43-57.

30. Y. Yamamato, T. Kamiya, and H. Yanai, "Characteristics of Optical Guided Modes in Multilayer Metal-Clad Planar Optical Guide with Low-Index Dielectric Buffer Layer," IEES J of Quantum Elec., Vol. QE-11, no. 9, September 1975, pp. 729-736.

31. T.E. Batchman and K.A. McMillan, "Measurement on Positive-Permittivity Metal-Clad Waveguides," IEEE J of Quantum Elec., Vol. A.E.-13, No. 4, April 1977.

32. T.E. Batchman and J.R. Peeler, "Gallium Arsenide Clad Optical Waveguides," IEEE J of Quantum Elec., Vol. Q.E.-14, No. 5, May 1978, pp. 327-329.

33. H.J. Fink, "Propagation of Waves in Optical Waveguides with Various Dielectric and Metal Claddings," IEEE J of Quantum Elec. (Corresp.), Vol. Q.E.-12, pp. 365-367, June 1976.

34. J.N. Polky and G.L. Mitchell, "Metal-clad Plannar Dielectric Waveguide for Integrated Optics," J. Opt. Soc. Amer., Vol. 64, pp. 274-279, March 1974.

35. A. Otto and W. Sohler, "Modification of the Total Reflection Modes in a Dielectric Film by One Metal Boundary," Opt. Commun., Vol. 3, pp. 254-255, June 1971.

36. R.A. Sprague and P. Nisenson, "The PROM-A Status Report," Optical Engineering, Vol. 17, No. 3, pp. 256-266, 1978.

37. H. Hayashi and Y. Fujii, "Programmable Optical Guided-Wave Device using Bi_{12} SiO_{20} Crystal," IEEE J of Quantum Electronics, Vol. QE-14, No. 11, pp. 848-854, 1978.

38. J.F. Brinton (reviewer), "Electronic Modulator Speeds up Processing for Optical Computer," Electronics, pp. 41-42, June 7, 1979.

39. J.Tauc, Amorphous and Liquid Semiconductors, Plenum Press, New York, p.231 and 346, 1974.

40. C.R. Wronski, "Electonic Properties of Amorphous Silicon in Solar Cell Operation," IEEE Tran. on Electron Devices, Vol. ED-24, No. 4, pp.351-357, April 1977.

41. J.I. Pankove and D.E. Carlson, "Electroluminescence in Amorphous Silicon," App. Phys. Lett., Vol. 29, No. 9. pp. 620-621, 1 Nov. 1976.

42. Stewart, Millar, Laybourn, Wilkinson and DelaRue, "Planar Optical Waveguides Formed by Silver-Ion Migration in Glass," IEEE J. Quantum Electronics, Vol. QE-13 (1977) pp. 192-200.

43. G. Stewart, and P. J. R. Laybourn, "Fabrication of Ion Exchanged Optical Waveguides From Dilute Silver Nitrate Melts," IEEE J. Quantum Electronics, Vol. Qe-14 (1978) pp. 930-934.

44. A. Gedeon, "Formation and Characteristics of Graded-Index Optical Waveguides Buried in Glass," Appl. Phys., Vol. 6 (1975), pp. 223-228.

45. Giallorenzi, West, Kirk, Ginther and Andrews, "Optical Waveguides Formed by Thermal Migration of Ions in Glass," Appl. Opt., Vol. 12 (1973), pp. 1240-1245.

46. I. Savatinova, "Lightguiding in Ion-Exchanged Glasses," Appl. Phys., Vol. 11 (1976) pp. 273-276.

APPENDIX A

PUBLICATIONS

The following papers were published during the time of this contract. The first paper appears in the Proceedings of Southeastcon '79 and the second paper will appear in the Proceedings of Southeastcon '80.

Waveguide Excitation of Optical Surface Waves for Metal-Barrier-Metal Devices

K.B. Gates T.E. Batchman

Department of Electrical Engineering
University of Virginia
Charlottesville, Va. 22901

Abstract

We consider the coupling of waveguide modes to surface waves on thin metal films and then the coupling to the metal-barrier-metal devices. It is shown that the TM_0 mode may couple to the surface wave using a four-layer waveguide where the metal film is more than 10 nanometers. Maxwell's Equations correctly predict the characteristics of thin film waveguides when the layer thicknesses are 10 nanometers or greater.

Metal-oxide-metal devices (MOMS) exhibiting an invariant I-V characteristic extending from DC up to optical frequencies have been fabricated and tested[1]. Even though the MOM devices are potentially very versatile, their applications at optical frequencies are limited because of the problems of coupling into the optical surface plasma wave. Gustafson indicates that coupling losses are due to losses of exciting the surface plasma mode, finite propagation distances of the surface plasma mode due to absorption by the metal, and scattering losses at the onset of the MOM[3]. Because of coupling problems, the MOM devices are being fabricated on the back of prisms; therefore, all applications are restricted to operations on free space waves. The full potential of the MOM device in light of present technology can be achieved only through the use of coupling to thin-film planar waveguides. The geometrical structure of the device lends itself to integrated optics in that both utilize the same fabrication technique and are thin-film structures. Devices have been fabricated and tested, demonstrating properties of amplification, modulation, and detection. The device's utility will only be realized by development of integrated optical coupling techniques.

The MOM device consists of approximately a one to two nanometers thick oxide placed between two metal films. When optical radiation is incident on the device, part of it is absorbed in the metal and part contributes to an electric field in the oxide. Device operation is believed to be from three mechanisms[1,2,3]: Fermi level modulation by the trapped electric field in the oxide, phonon assisted electron tunneling through the oxide due to phonon creation by incident photons, and direct optical exitation of electron tunneling. In treating the device as a waveguide, it has been found that neither TE nor TM modes will propagate through the device since the oxide is below cutoff thickness for symmetrical metal-clad waveguides[4]; however, surface plasma modes are excited on each metal. The existence of these surface plasma modes at interfaces of metals and dielectrics have been predicted and studied[5,6]. These surface modes lead to the formation of symmetric and antisymmetric gap plasma modes in the device. If the antisymmetric mode is excited, then Fermi level modulation of tunneling electrons takes place. Since the oxide is so thin, transition times for tunneling electrons are on the order of 10^{-16} sec.[1] which allows for transition frequencies up to 10^{16} Hertz or light frequencies. Even though surface plasma wave amplification mechanisms are not completely understood at this time, the process has been theorized to exist and has recently been demonstrated[1].

The MOM device is a section of a symmetric metal clad three layer waveguide where the oxide is extremely thin. It has been suggested that MOM's can be placed on the same chip along with other integrated components and interconnecting planar slab waveguides. The coupling structure in this paper is a modification to a four layer waveguide since this structure already contains one electrode and a second electrode may be introduced by making it a symmetrical five-layer waveguide. In such a coupler the basic guiding dielectric core would become thinner and thinner to couple TM (transverse magnetic) modes to surface plasma modes.

An extensive analysis of the asymmetric four layer waveguide and their supported propagating modes has been done[4,5,6,7]. This procedure consisted of solving Maxwell's Equations for the dispersion relations and then generating a computer program for numerically solving the transcendental relation. Various metal and semiconductor clad waveguides have been analyzed and the effect of varying waveguide parameters such as film thicknesses and the material permitivities on propagating modes have been established.

A comparison of the three layer dielectric guide and a four layer guide with a metal film inserted between the substrate and the guiding dielectric demonstrates that the inclusion of the thin metal film changes the mode profile for TM modes appreciably yet the effect on the TE modes is only slight. Figure 1 shows the field distribution after a thin metal film has been introduced.

CH1432-4/79/0000-0104$00.75

Rashleigh[4] has hypothesized that the field concentration in the metal gives rise to the TM_0 mode coupling to the surface plasma mode. This hypothesis is supported by comparing the surface wave field distribution, Fig. 2, to that of Fig. 1 for the TM_0 mode.

The conclusion from this analysis is that TE modes do not couple to the surface plasma modes because there is no concentration of field strength at the metal-dielectric interface where the TM' mode exists. The TM mode field concentration at this interface increases as mode order is reduced. The computer solution technique method mapped out previously predicts the existence of the TM' mode in that there is extreme attenuation found in the TM modes; this is much higher than expected. The rational is that the TM modes are coupling into a highly attenuated surface plasma mode and thus they are highly attenuated. As the concentration of the field in the metal increases so does the attenuation.

TM mode coupling to the surface plasma wave appears feasible when the variation or mode index with metal thickness is compared for the TM_0 and TM' modes. When the TM_0 mode index is near the TM' mode index greater coupling should occur and thus the TM_0 mode will be attenuatad accordingly. When the TM_0 mode index is close to the TM' mode index, guide attenuation is high. As the metal thickness is reduced, the TM_0 mode index draws away from the TM' mode index and the attenuation is reduced. A similar effect would be to change the core dielectric to vary the mode index of the TM modes. Again attenuation is expected to increase as the TM mode indices become closer to the surface plasma mode index.

Based on a quantum mechanical derivation of Maxwell's Equations[8] the limit at which these equations are no longer valid are film thickness of 10 nanometers. A quantum mechanical analysis of thinner films was deemed unnecessary since surface fluctuations of thin films are on the order of 7-8 nonometers with present technology. There are several papers which have stretched Maxwell's Equations down to below this theoretical and practical limit[5]. Maxwell's Equations are valid down to the limit of 10 nanometers and below this thickness, theoretical analyses to date are not applicable.

In conclusion, coupling to the MOM device from optical waveguides must be realized with films of 10 nanometers or greater. We believe that this can be achieved with the coupling structure outlined.

References

1. M. Herbluin, et al, Optical Communication Systemr, Rpt. of a Grantee-User Meeting at Columbia Univ., New York City, 49, (1977).
2. D.P. Siu and T.K. Gustafson, Appl. Phys. Lett. 32(8), 500, (1978).
3. T.K. Gustafson, Optical Communication Systems, Proceedings of NSF Grantee-User Meeting, Pittsburgh, Pa., 148, (1978).
4. S.C. Rashleigh, Ph.D. Thesis, University of Queensland, Brisbane, Australia, May 1975.
5. Y. Yamamoto, et al, IEEE J. Q.E., QE11, No.9, 729 (1975).
6. T.E. Batchman and K.A. McMillan, IEEE J. Q.E., QE13, No.4, (1977).
7. T.E. Batchman and J.R. Peeler, IEEE J. Q.E., QE14, No.5, 327, (1978).
8. J.P. Jackson, Classical Electrodynamics, John Wiley & Sons, Inc., New York, 1975, pp. 226-235.

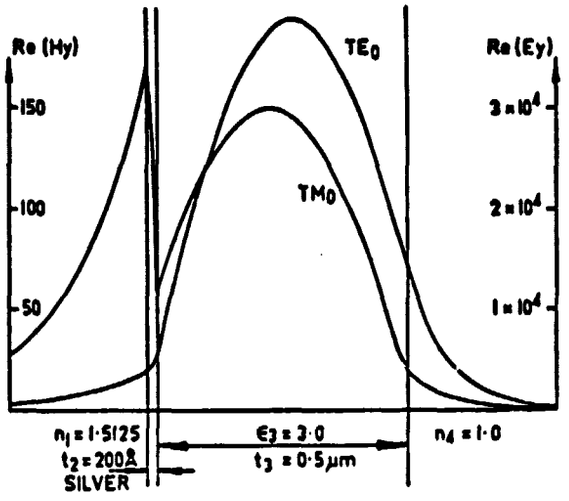

Fig. 1 Fields of propagating modes in a metal-clad waveguide

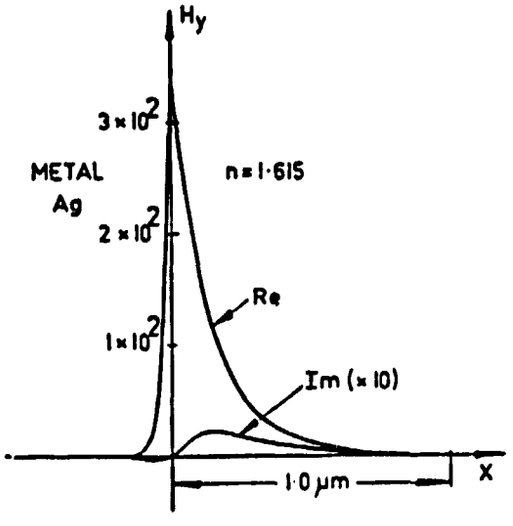

Fig. 2 Surface plasma mode field distribution

Semiconductor Clad Optical Waveguides

K. Gates, D. Summers and T.E. Batchman

University of Virginia
Electrical Engineering Department
Charlottesville, VA 22901

ABSTRACT

At a free space wavelength of 633 nanometers, semiconductor clad waveguides are investigated. Calculations show that the waveguide attenuation coefficient (α) and the propagation coefficient (β) vary with semiconductor thickness similar to a damped harmonic of period 80 nanometers. The complex semiconductor index of refraction relegates curve damping and amplitude factors. Three of the more common semiconductors (Si, Ge, GaAs) have been investigated as cladding materials and results are discussed.

INTRODUCTION

Planar multi-layer dielectric optical waveguides have been studied extensively using various materials for the waveguides and cladding regions.[1] We have extended previous analysis to include the case of a buffer region being a thin semiconductor film. Maxwell's equations and boundary conditions were used to derive a transcendental equation relating the propagation constant of a guided mode to waveguide parameters. Over several years, a computer program has evolved to numerically solve this complex transcendental equation for the complex mode propagation constant ($\alpha + j\beta$). In the case of three or more dielectric layers, the permittivities (refractive index) are real, α is zero and thus the semiconductor cladding has a conductivity at optical frequencies which gives rise to an imaginary part of the permittivity ($\epsilon = \epsilon' + j\frac{\sigma}{\omega}$), and α becomes non-zero.[3]

Semiconductor Clad Waveguides

The optical waveguide under consideration here is a planar, four layer slab waveguide. Propagation of light is assumed to be in the z-direction and material variations occur in the x-direction only. The waveguide is composed of a semi-infinate glass substrate, a polystyrene core of thickness 1.0 micrometer, a semiconductor cladding of 0.01 to 10 micrometers in thickness and a semi-infinate layer of air. A free-space wavelength of 633 nanometers was assumed and thus all material parameters are for this wavelength. The three most common semiconductors, gallium arsenide, silicon and germanium were used as the cladding layer. For a discussion of metal and semiconductor clad waveguides see references 3, 4, 5, 6, 7, 8 and 9.

Assuming all materials except the semiconductor are lossless, the waveguide is constant in the y and z directions, and refractive index varies in a step function profile in the x direction, we apply Maxwell's field equations to generate a wave equation. The problem separates into transverse electric and transverse magnetic cases. By determining the non-zero field components, invoking continuity of the wave function and forcing the field components to satisfy Maxwell's boundary conditions, a dispersion relation for each propagating mode is obtained that relates α and β, the attenuation and phase constants, respectively, to the waveguide material and structural parameters. These dispersion relations are complex transcendental equations which must be solved iteratively using a computer program.

At optical frequencies, the refractive index of a semiconductor is complex. Permittivity becomes complex ($\epsilon = \epsilon' + j\epsilon''$) when the conductivity becomes significant, $\epsilon'' = 4\pi\sigma/\omega$. The complex part of the permittivity is a linear function of the conductivity which can be externally varied. Table I presents the permittivity and refractive index for the three main semiconductors. The real part of the permittivities for all three are approximately the same and the complex part for germanium is an order of magnitude greater than that of gallium arsenide and silicon.

Table I

Semiconductor Parameters at λ = 632.8 nm

Material	Permittivity ϵ'	Permittivity ϵ''	Refractive Index n	Refractive Index k
GaAs	14.3	1.21	3.79	0.16
Silicon*	16.76	0.87	4.1	0.213
Germanium*	14.43	9.77	4.4	2.22

*values for amorphous thin films

Predicted Characteristics

Choosing gallium arsenide as the cladding semiconductor, the curves presented in Fig. 1 and Fig. 2 were generated by repetative use of the previously mentioned program. The cladding thickness was varied from .01 to 10 micrometers. The expected result was as the cladding thickness is reduced to zero the attenuation would decrease to zero in a well-behaved manner. However the results are not well-behaved when the cladding thickness falls below 1.0 micrometer. The curves are similar to exponentially damped sinusoids. The extreme β/k variations correspond to median values in the α-curve and extreme α variations correspond to median β/k values. By increasing the conductivity of the gallium arsenide cladding, the amplitude of the curve oscillations were reduced and the α-curve shifted slightly towards a higher attenuation. This result was expected since a greater conductivity increases material absorbtion of energy and therefore a higher attenuation in the propagating wave, yet at the maximum points there was actually a decrease in the attenuation.

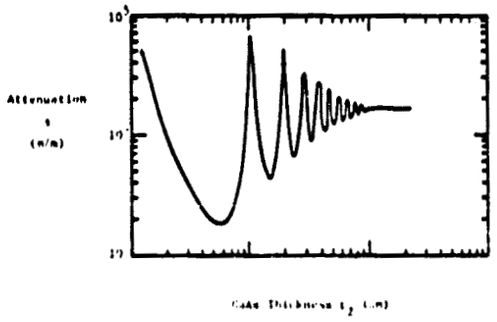

Fig. 1 - GaAs/AIR-CLAD WAVEGUIDE ATTENUATION vs t_2 (TE_0 MODE, NORMAL CONDUCTIVITY; t_3 = 0.8 μm)

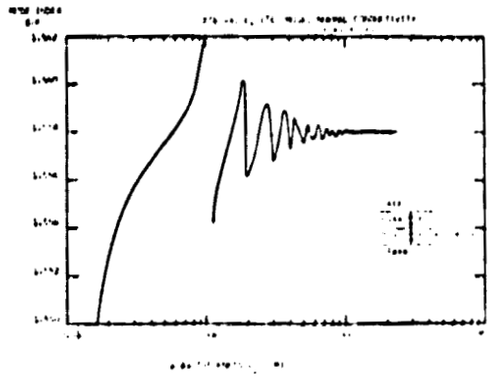

FIG. 2 - MODE INDEX OF GaAs CLAD WAVEGUIDE

Silicon clad waveguides maintained all the properties of the gallium arsenide clad waveguides. Fig. 3 and Fig. 4 present the computer predictions based on a core thickness of 1.0 micrometers. The curves are nearly identical with the curves generated using gallium arsenide as the cladding. The oscillations are damped out at a cladding thickness of 1.0 micrometers. Variations on the conduccivity reproduced the affects found for the previous case.

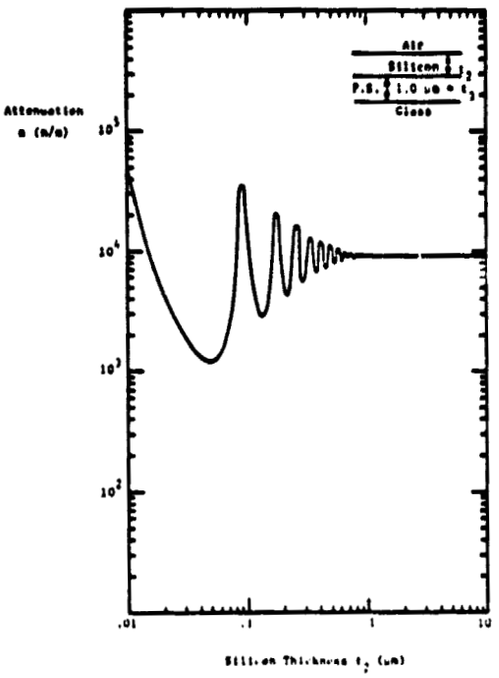

Fig. 3 - SILICON/AIR CLAD GUIDE ATTENUATION vs t_2 (TE_0 MODE, NORMAL CONDUCTIVITY)

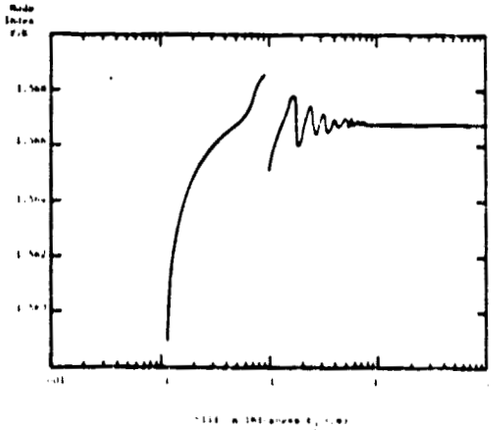

FIG. 4 - SILICON/AIR CLAD GUIDE β/K vs t_2 (TE_0 MODE, NORMAL CONDUCTIVITY)

The cladding semiconductor was changed to germanium and the oscillations in the attenuation and normalized phase curves disappeared, Fig. 5 and Fig. 6. These results are attributed to the greater conductivity of germanium.

In reference 2, the author considered a thin film of material with $n = 2$ and k ($k = \alpha\lambda/4\pi$) varying and he calculated the expected phase change on reflection of an incident wave at an air-film surface. For k very small, the phase change was found to oscillate while for k large, the phase changed very little until the film thickness approached zero. This behavior has also been predicted by Stratton [12] and is like the effect we have observed here.

The proposed explanation for the results is that there is an interference effect across the waveguide and when constructive interference occurs in the semiconductor cladding, the propagating wave field strength in the cladding will be greater and a higher attenuation is expected. Likewise, destructive interference will cause a much lower attenuation. Normalized phase shifts must be at a maximum when the interference effects are at a minimum, similar to the results of transmission calculations of waves through an absorbing medium. Increasing the conductivity of the semiconductor cladding increases the field strength attenuation in the cladding which decreases the effect of the interference. At the points where a greater conductivity causes a lower attenuation the greater conductivity increases the reflection at the cladding-core interface and thus there is less field strength in the absorbing medium and less attenuation in the propagating wave.

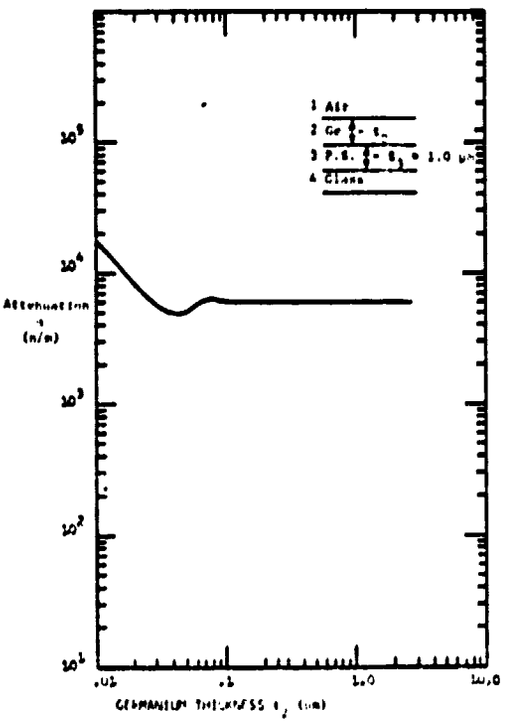

Fig. 5 - GERMANIUM/AIR CLAD GUIDE ATTENUATION vs t_2 (TE_0 MODE, NORMAL CONDUCTIVITY)

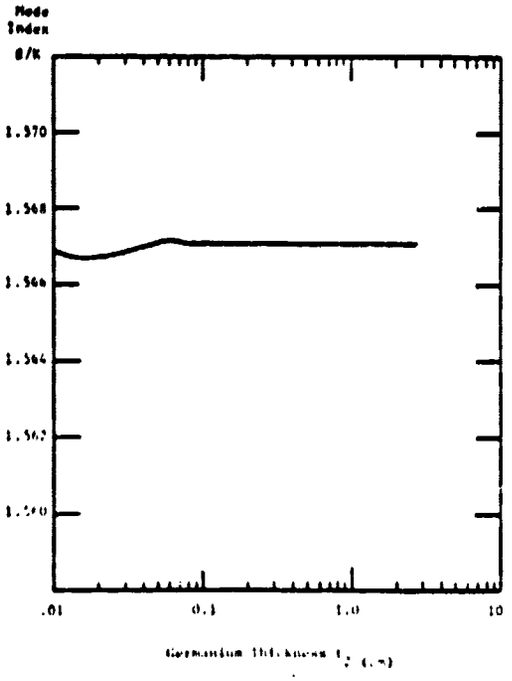

Fig. 6 - GERMANIUM/AIR CLAD GUIDE, β/k vs t_2 (TE_0 MODE; NORMAL CONDUCTIVITY)

A plausible device utilizing these results would be either a guided light wave amplitude modulator or phase modulator. To amplitude modulate, the semiconductor cladding would be either gallium arsenide or silicon and of such thickness that there was maximum amplitude change with minimum phase change as the conductivity is varied. Any of the minimum points on the α-curves could be selected and the modulator thickness thus determined. To modulate, the semiconductor conductivity must be varied, which can be done through any of a variety of means such as by heat, electric fields and incident light.

Thin films of amorphous silicon have been fabricated [10,11] and measured conductivities have been as much as several orders of magnitude lower than the conductivity value used in Table I for this study. The conductivity of amorphous silicon varies greatly due to differences in fabrication procedures and thermal histories. It is expected that the attenuation curve mean value will be lower and the oscillations of both α and β/k curves will be increased in magnitude when amorphous films are fabricated.

This study is not complete at this time. Amorphous silicon has not been completely investigated and field plots of the propagating wave in the waveguide have yet to be developed.

Conclusion

A device has been proposed and laboratory experiments are presently being conducted to verify the theoretical predictions. A planar waveguide with a wedged shaped silicon cladding across the width should demonstrate the damped oscillations in the attenuation curves and conductivity variations of the silicon should demonstrate the modulation capabilities.

References

1 I.P. Kaminow, W.L. Mammel, and H.P. Weber, "Metal-clad optical waveguides: Analytical and experimental study," Appl. Opt., Vol. 13, pp. 396-405.

2 O.S. Heavens, Optical Properties of Thin Solid Films, Academic Press, Inc. New York, 1955, pp. 170-172.

3 S.C. Rashleigh, Planar Metal-Clad Dielectric Optical Waveguides, Phd Thesis, University of Queensland, Brisbane Australia, May 1975, pp. 199-200.

4 P.K. Tien and R.J. Martin, "Experiments on Light Waves in a Thin Tapered Film and a New Light-Wave Coupler," Applied Physics Letters, Vol. 18, May 1, 1971, pp. 398-401.

5 Y. Yamamoto, T. Kamiya, and H. Yanai, "Characteristics of Optical Guided Modes in Multilayer Metal-Clad Planar Optical Guide with Low-Index Dielectric Buffer Layer," IEEE J of Quantum Elec., Vol. QE-11, no. 9, September 1975, pp. 729-736.

6 T.E. Batchman and D.A. McMillan, "Measurement on Positive-Permittivity Metal-Clad Waveguides," IEEE J of Quantum Elec., Vol. A. E.-13, No. 4, April 1977.

7 T.E. Batchman and J.K. Peeler, "Gallium Arsenide Clad Optical Waveguides," IEEE J of Quantum Elec., Vol. Q. E.-14, No. 5, May 1978, pp. 327-329.

8 M.J. Fink, "Propagation of Waves in Optical Waveguides with Various Dielectric and Metal Claddings," IEEE J of Quantum Elec. (Corresp.), Vol. Q.E.-12, pp. 365-367, June 1976.

9 J.N. Polky and G.L. Mitchell, "Metal-clad Planner Dielectric Waveguide for Integrated Optics," J. Opt. Soc. Amer., Vol. 64, pp. 274-279, March 1974.

10 J. Tauc, Amorphous and Liquid Semiconductors, Plenum Press, New York, P. 231 and 346, 1974.

11 C.R. Wronski, "Electronic Properties of Amorphous Silicon in Solar Cell Operation," IEEE Tran. on Electron Devices, Vol. ED-24, No. 4, pp. 351-357, April 1977.

12 J.D. Stratton, Electromagnetic Theory, McGraw-Hill Book Co., New York, pp. 515-516, 1941.

APPENDIX A

PUBLICATIONS

The following papers were published during the time of this contract. The first paper appears in the Proceedings of Southeastcon '79 and the second paper will appear in the Proceedings of Southeastcon '80.

Waveguide Excitation of Optical Surface Waves for Metal-Barrier-Metal Devices

K.B. Gates T.E. Batchman

Department of Electrical Engineering
University of Virginia
Charlottesville, Va. 22901

Abstract

We consider the coupling of waveguide modes to surface waves on thin metal films and then the coupling to the metal-barrier-metal devices. It is shown that the TM_0 mode may couple to the surface wave using a four-layer waveguide where the metal film is more than 10 nanometers. Maxwell's Equations correctly predict the characteristics of thin film waveguides when the layer thicknesses are 10 nanometers or greater.

Metal-oxide-metal devices (MOMS) exhibiting an invariant I-V characteristic extending from DC up to optical frequencies have been fabricated and tested[1]. Even though the MOM devices are potentially very versatile, their applications at optical frequencies are limited because of the problems of coupling into the optical surface plasma wave. Gustafson indicates that coupling losses are due to losses of exciting the surface plasma mode, finite propagation distances of the surface plasma mode due to absorption by the metal, and scattering losses at the onset of the MOM[3]. Because of coupling problems, the MOM devices are being fabricated on the back of prisms; therefore, all applications are restricted to operations on free space waves. The full potential of the MOM device in light of present technology can be achieved only through the use of coupling to thin-film planar waveguides. The geometrical structure of the device lends itself to integrated optics in that both utilize the same fabrication technique and are thin-film structures. Devices have been fabricated and tested, demonstrating properties of amplification, modulation, and detection. The device's utility will only be realized by development of integrated optical coupling techniques.

The MOM device consists of approximately a one to two nanometers thick oxide placed between two metal films. When optical radiation is incident on the device, part of it is absorbed in the metal and part contributes to an electric field in the oxide. Device operation is believed to be from three mechanisms[1,2,3]: Fermi level modulation by the trapped electric field in the oxide, phonon assisted electron tunneling through the oxide due to phonon creation by incident photons, and direct optical exitation of electron tunneling. In treating the device as a waveguide, it has been found that neither TE nor TM modes will propagate through the device since the oxide is below cutoff thickness for symmetrical metal-clad waveguides[4]; however, surface plasma modes are excited on each metal. The existence of these surface plasma modes at interfaces of metals and dielectrics have been predicted and studied[5,6]. These surface modes lead to the formation of symmetric and antisymmetric gap plasma modes in the device. If the antisymmetric mode is excited, then Fermi level modulation of tunneling electrons takes place. Since the oxide is so thin, transition times for tunneling electrons are on the order of 10^{-16} sec.[1] which allows for transition frequencies up to 10^{16} Hertz or light frequencies. Even though surface plasma wave amplification mechanisms are not completely understood at this time, the process has been theorized to exist and has recently been demonstrated[1].

The MOM device is a section of a symmetric metal clad three layer waveguide where the oxide is extremely thin. It has been suggested that MOM's can be placed on the same chip along with other integrated components and interconnecting planar slab waveguides. The coupling structure in this paper is a modification to a four layer waveguide since this structure already contains one electrode and a second electrode may be introduced by making it a symmetrical five-layer waveguide. In such a coupler the basic guiding dielectric core would become thinner and thinner to couple TM (transverse magnetic) modes to surface plasma modes.

An extensive analysis of the asymmetric four layer waveguide and their supported propagating modes has been done[4,5,6,7]. This procedure consisted of solving Maxwell's Equations for the dispersion relations and then generating a computer program for numerically solving the transcendental relation. Various metal and semiconductor clad waveguides have been analyzed and the effect of varying waveguide parameters such as film thicknesses and the material permitivities on propagating modes have been established.

A comparison of the three layer dielectric guide and a four layer guide with a metal film inserted between the substrate and the guiding dielectric demonstrates that the inclusion of the thin metal film changes the mode profile for TM modes appreciably yet the effect on the TE modes is only slight. Figure 1 shows the field distribution after a thin metal film has been introduced.

CH1432-4/79/0000-0104$00.75

Rashleigh[4] has hypothesized that the field concentration in the metal gives rise to the TM_0 mode coupling to the surface plasma mode. This hypothesis is supported by comparing the surface wave field distribution, Fig. 2, to that of Fig. 1 for the TM_0 mode.

The conclusion from this analysis is that TE modes do not couple to the surface plasma modes because there is no concentration of field strength at the metal-dielectric interface where the TM' mode exists. The TM mode field concentration at this interface increases as mode order is reduced. The computer solution technique method mapped out previously predicts the existence of the TM' mode in that there is extreme attenuation found in the TM modes; this is much higher than expected. The rational is that the TM modes are coupling into a highly attenuated surface plasma mode and thus they are highly attenuated. As the concentration of the field in the metal increases so does the attenuation.

TM mode coupling to the surface plasma wave appears feasible when the variation or mode index with metal thickness is compared for the TM_0 and TM' modes. When the TM_0 mode index is near the TM' mode index greater coupling should occur and thus the TM_0 mode will be attenuatad accordingly. When the TM_0 mode index is close to the TM' mode index, guide attenuation is high. As the metal thickness is reduced, the TM_0 mode index draws away from the TM' mode index and the attenuation is reduced. A similar effect would be to change the core dielectric to vary the mode index of the TM modes. Again attenuation is expected to increase as the TM mode indices become closer to the surface plasma mode index.

Based on a quantum mechanical derivation of Maxwell's Equations[8] the limit at which these equations are no longer valid are film thickness of 10 nanometers. A quantum mechanical analysis of thinner films was deemed unnecessary since surface fluctuations of thin films are on the order of 7-8 nonometers with present technology. There are several papers which have stretched Maxwell's Equations down to below this theoretical and practical limit[5]. Maxwell's Equations are valid down to the limit of 10 nanometers and below this thickness, theoretical analyses to date are not applicable.

In conclusion, coupling to the MOM device from optical waveguides must be realized with films of 10 nanometers or greater. We believe that this can be achieved with the coupling structure outlined.

References

1. M. Herbluin, et al, Optical Communication Systemr, Rpt. of a Grantee-User Meeting at Columbia Univ., New York City, 49, (1977).
2. D.P. Siu and T.K. Gustafson, Appl. Phys. Lett. 32(8), 500, (1978).
3. T.K. Gustafson, Optical Communication Systems, Proceedings of NSF Grantee-User Meeting, Pittsburgh, Pa., 148, (1978).
4. S.C. Rashleigh, Ph.D. Thesis, University of Queensland, Brisbane, Australia, May 1975.
5. Y. Yamamoto, et al, IEEE J. Q.E., QE11, No.9, 729 (1975).
6. T.E. Batchman and K.A. McMillan, IEEE J. Q.E., QE13, No.4, (1977).
7. T.E. Batchman and J.R. Peeler, IEEE J. Q.E., QE14, No.5, 327, (1978).
8. J.P. Jackson, Classical Electrodynamics, John Wiley & Sons, Inc., New York, 1975, pp. 226-235.

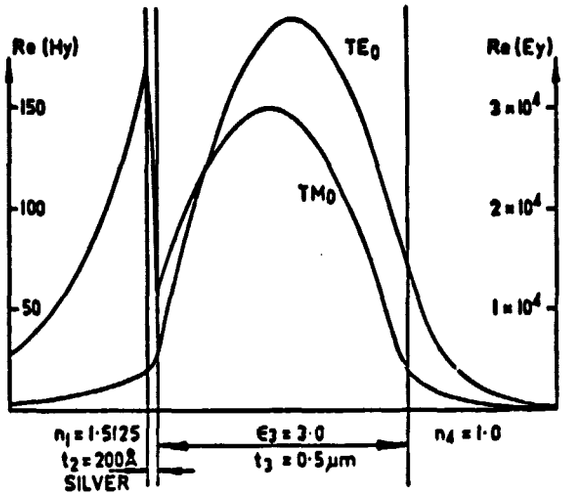

Fig. 1 Fields of propagating modes in a metal-clad waveguide

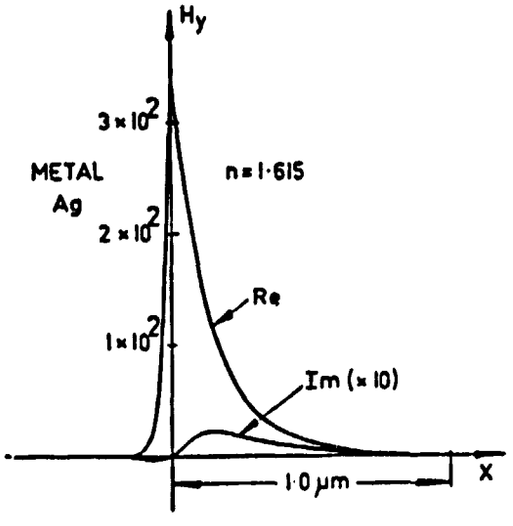

Fig. 2 Surface plasma mode field distribution

Semiconductor Clad Optical Waveguides

K. Gates, D. Summers and T.E. Batchman

University of Virginia
Electrical Engineering Department
Charlottesville, VA 22901

ABSTRACT

At a free space wavelength of 633 nanometers, semiconductor clad waveguides are investigated. Calculations show that the waveguide attenuation coefficient (α) and the propagation coefficient (β) vary with semiconductor thickness similar to a damped harmonic of period 80 nanometers. The complex semiconductor index of refraction relegates curve damping and amplitude factors. Three of the more common semiconductors (Si, Ge, GaAs) have been investigated as cladding materials and results are discussed.

INTRODUCTION

Planar multi-layer dielectric optical waveguides have been studied extensively using various materials for the waveguides and cladding regions.[1] We have extended previous analysis to include the case of a buffer region being a thin semiconductor film. Maxwell's equations and boundary conditions were used to derive a transcendental equation relating the propagation constant of a guided mode to waveguide parameters. Over several years, a computer program has evolved to numerically solve this complex transcendental equation for the complex mode propagation constant ($\alpha + j\beta$). In the case of three or more dielectric layers, the permittivities (refractive index) are real, σ is zero and thus the semiconductor cladding has a conductivity at optical frequencies which gives rise to an imaginary part of the permittivity ($\epsilon = \epsilon' + j\epsilon''$), and α becomes non-zero.[3]

Semiconductor Clad Waveguides

The optical waveguide under consideration here is a planar, four layer slab waveguide. Propagation of light is assumed to be in the z-direction and material variations occur in the x-direction only. The waveguide is composed of a semi-infinate glass substrate, a polystyrene core of thickness 1.0 micrometer, a semiconductor cladding of 0.01 to 10 micrometers in thickness and a semi-infinate layer of air. A free-space wavelength of 633 nanometers was assumed and thus all material parameters are for this wavelength. The three most common semiconductors, gallium arsenide, silicon and germanium were used as the cladding layer. For a discussion of metal and semiconductor clad waveguides see references 3, 4, 5, 6, 7, 8 and 9.

Assuming all materials except the semiconductor are lossless, the waveguide is constant in the y and z directions, and refractive index varies in a step function profile in the x direction, we apply Maxwell's field equations to generate a wave equation. The problem separates into transverse electric and transverse magnetic cases. By determining the non-zero field components, invoking continuity of the wave function and forcing the field components to satisfy Maxwell's boundary conditions, a dispersion relation for each propagating mode is obtained that relates α and β, the attenuation and phase constants, respectively, to the waveguide material and structural parameters. These dispersion relations are complex transcendental equations which must be solved iteratively using a computer program.

At optical frequencies, the refractive index of a semiconductor is complex. Permittivity becomes complex ($\epsilon = \epsilon' + j\epsilon''$) when the conductivity becomes significant, $\epsilon'' = 4\pi\sigma/\omega$. The complex part of the permittivity is a linear function of the conductivity which can be externally varied. Table I presents the permittivity and refractive index for the three main semiconductors. The real part of the permittivities for all three are approximately the same and the complex part for germanium is an order of magnitude greater than that of gallium arsenide and silicon.

Table I

Semiconductor Parameters at λ = 632.8 nm

Material	Permittivity ϵ'	Permittivity ϵ''	Refractive Index n	Refractive Index k
GaAs	14.1	1.21	3.79	0.16
Silicon*	16.76	0.87	4.1	0.213
Germanium*	14.43	9.77	4.4	2.22

*values for amorphous thin films

Predicted Characteristics

Choosing gallium arsenide as the cladding semiconductor, the curves presented in Fig. 1 and Fig. 2 were generated by repetative use of the previously mentioned program. The cladding thickness was varied from .01 to 10 micrometers. The expected result was as the cladding thickness is reduced to zero the attenuation would decrease to zero in a well-behaved manner. However the results are not well-behaved when the cladding thickness falls below 1.0 micrometer. The curves are similar to exponentially damped sinusoids. The extreme β/k variations correspond to median values in the α-curve and extreme α variations correspond to median β/k values. By increasing the conductivity of the gallium arsenide cladding, the amplitude of the curve oscillations were reduced and the α-curve shifted slightly towards a higher attenuation. This result was expected since a greater conductivity increases material absorbtion of energy and therefore a higher attenuation in the propagating wave, yet at the maximum points there was actually a decrease in the attenuation.

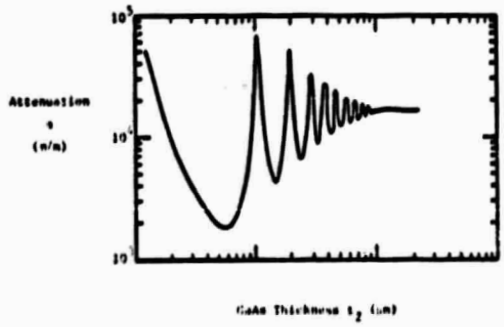

Fig. 1 - GaAs/AIR-CLAD WAVEGUIDE ATTENUATION vs t_2 (TE_0 MODE, NORMAL CONDUCTIVITY; t_3 = 0.8 μm)

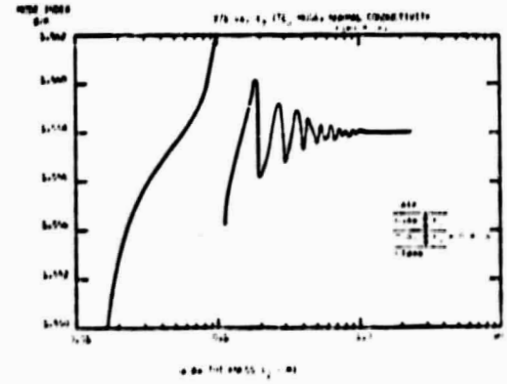

Fig. 2 - MODE INDEX OF GaAs CLAD WAVEGUIDE

Silicon clad waveguides maintained all the properties of the gallium arsenide clad waveguides. Fig. 3 and Fig. 4 present the computer predictions based on a core thickness of 1.0 micrometers. The curves are nearly identical with the curves generated using gallium arsenide as the cladding. The oscillations are damped out at a cladding thickness of 1.0 micrometers. Variations on the conductivity reproduced the affects found for the previous case.

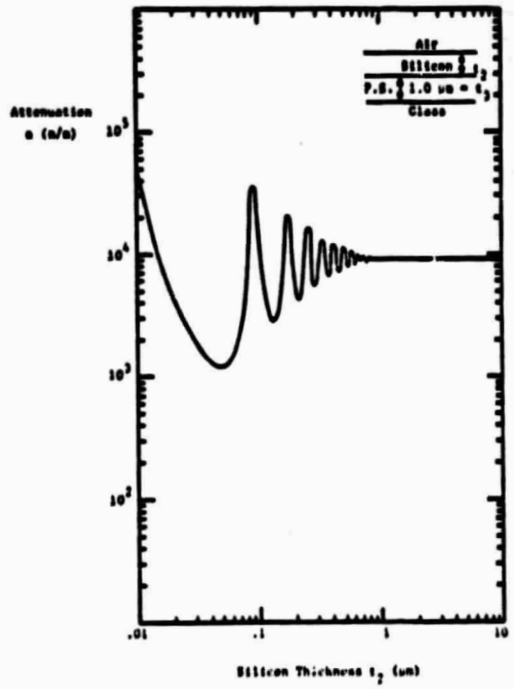

Fig. 3 - SILICON/AIR CLAD GUIDE ATTENUATION vs t_2 (TE_0 MODE, NORMAL CONDUCTIVITY)

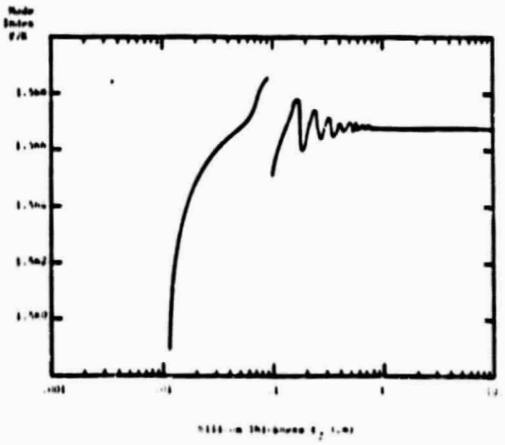

Fig. 4 - SILICON/AIR CLAD GUIDE β/K vs t_2 (TE_0 MODE, NORMAL CONDUCTIVITY)

The cladding semiconductor was changed to germanium and the oscillations in the attenuation and normalized phase curves disappeared, Fig. 5 and Fig. 6. These results are attributed to the greater conductivity of germanium.

In reference 2, the author considered a thin film of material with $\eta = 2$ and k ($k = \alpha\lambda/4\pi$) varying and he calculated the expected phase change on reflection of an incident wave at an air-film surface. For k very small, the phase change was found to oscillate while for k large, the phase changed very little until the film thickness approached zero. This behavior has also been predicted by Stratton [12] and is like the effect we have observed here.

The proposed explanation for the results is that there is an interference effect across the waveguide and when constructive interference occurs in the semiconductor cladding, the propagating wave field strength in the cladding will be greater and a higher attenuation is expected. Likewise, destructive interference will cause a much lower attenuation. Normalized phase shifts must be at a maximum when the interference effects are at a minimum, similar to the results of transmission calculations of waves through an absorbing medium. Increasing the conductivity of the semiconductor cladding increases the field strength attenuation in the cladding which decreases the effect of the interference. At the points where a greater conductivity causes a lower attenuation the greater conductivity increases the reflection at the cladding-core interface and thus there is less field strength in the absorbing medium and less attenuation in the propagating wave.

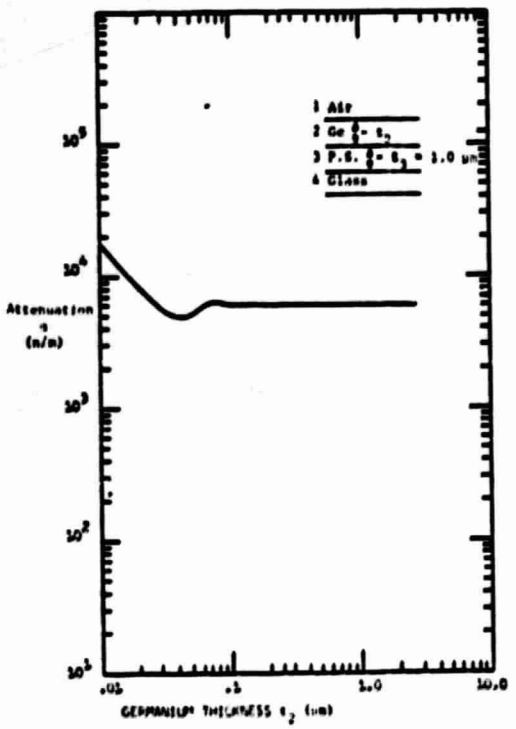

FIG. 5 - GERMANIUM/AIR CLAD GUIDE ATTENUATION vs t_2 (TE_0 MODE, NORMAL CONDUCTIVITY)

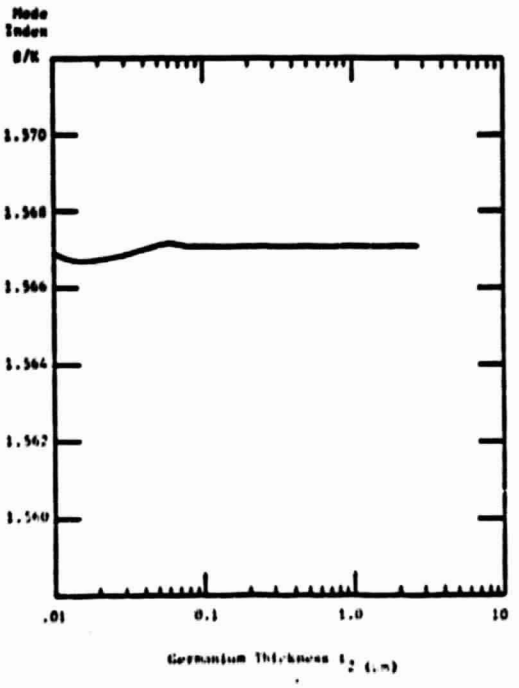

FIG. 6 - GERMANIUM/AIR CLAD GUIDE, β/k vs t_2 (TE MODE; NORMAL CONDUCTIVITY)

A plausible device utilizing these results would be either a guided light wave amplitude modulator or phase modulator. To amplitude modulate, the semiconductor cladding would be either gallium arsenide or silicon and of such thickness that there was maximum amplitude change with minimum phase change as the conductivity is varied. Any of the minimum points on the α-curves could be selected and the modulator thickness thus determined. To modulate, the semiconductor conductivity must be varied, which can be done through any of a variety of means such as by heat, electric fields and incident light.

Thin films of amorphous silicon have been fabricated [10,11] and measured conductivities have been as much as several orders of magnitude lower than the conductivity value used in Table I for this study. The conductivity of amorphous silicon varies greatly due to differences in fabrication procedures and thermal histories. It is expected that the attenuation curve mean value will be lower and the oscillations of both α and β/k curves will be increased in magnitude when amorphous films are fabricated.

This study is not complete at this time. Amorphous silicon has not been completely investigated and field plots of the propagating wave in the waveguide have yet to be developed.

Conclusion

A device has been proposed and laboratory experiments are presently being conducted to verify the theoretical predictions. A planar waveguide with a wedged shaped silicon cladding across the width should demonstrate the damped oscillations in the attenuation curves and conductivity variations of the silicon should demonstrate the modulation capabilities.

References

1 I.P. Kaminow, W.L. Mammel, and H.P. Weber, "Metal-clad optical waveguides: Analytical and experimental study," Appl. Opt., Vol. 13, pp. 396-405.

2 O.S. Heavens, Optical Properties of Thin Solid Films, Academic Press, Inc. New York, 1955, pp. 170-172.

3 S.C. Rashleigh, Planar Metal-Clad Dielectric Optical Waveguides, Phd Thesis, University of Queensland, Brisbane Australia, May 1975, pp. 199-200.

4 P.K. Tien and R.J. Martin, "Experiments on Light Waves in a Thin Tapered Film and a New Light-Wave Coupler," Applied Physics Letters, Vol. 18, May 1, 1971, pp. 398-401.

5 Y. Yamamoto, T. Kamiya, and H. Yanai, "Characteristics of Optical Guided Modes in Multilayer Metal-Clad Planar Optical Guide with Low-Index Dielectric Buffer Layer," IEEE J of Quantum Elec., Vol. QE-11, no. 9, September 1975, pp. 729-736.

6 T.E. Batchman and D.A. McMillan, "Measurement on Positive-Permittivity Metal-Clad Waveguides," IEEE J of Quantum Elec., Vol. A. E.-13, No. 4, April 1977.

7 T.E. Batchman and J.K. Peeler, "Gallium Arsenide Clad Optical Waveguides," IEEE J of Quantum Elec., Vol. Q. E.-14, No. 5, May 1978, pp. 327-329.

8 H.J. Fink, "Propagation of Waves in Optical Waveguides with Various Dielectric and Metal Claddings," IEEE J of Quantum Elec. (Corresp.), Vol. Q.E.-12, pp. 365-367, June 1976.

9 J.M. Polky and G.L. Mitchell, "Metal-clad Plannar Dielectric Waveguide for Integrated Optics," J. Opt. Soc. Amer., Vol. 64, pp. 274-279, March 1974.

10 J. Tauc, Amorphous and Liquid Semiconductors, Plenum Press, New York, P. 231 and 346, 1974.

11 C.R. Wronski, "Electronic Properties of Amorphous Silicon in Solar Cell Operation," IEEE Tran. on Electron Devices, Vol. ED-24, No. 4, pp. 351-357, April 1977.

12 J.D. Stratton, Electromagnetic Theory, McGraw-Hill Book Co., New York, pp. 515-516, 1941.